Universidade de Aveiro Departamento de Química
2016

CELINA RODRIGUES DE OLIVEIRA

CRISTALIZAÇÃO DE VITAMINA D_3 EM CONTÍNUO

CRYSTALLIZATION OF VITAMIN D_3 IN CONTINUOUS FLOW

Universidade de Aveiro Departamento de Química
2016

CELINA RODRIGUES DE OLIVEIRA

CRISTALIZAÇÃO DE VITAMINA D_3 EM CONTÍNUO

CRYSTALLIZATION OF VITAMIN D_3 IN CONTINUOUS FLOW

Dissertação apresentada à Universidade de Aveiro para cumprimento dos requisitos necessários à obtenção do grau de Mestre em Engenharia Química, realizada sob a orientação científica do Professor Doutor Volker Hessel, Professor do Departamento de Engenharia Química da Universidade de Tecnologia de Eindhoven, e do Professor Doutor Carlos Manuel Silva, Professor Auxiliar do Departamento de Química da Universidade de Aveiro.

o júri

Prof.ª Doutora Maria Inês Purcell de Portugal Branco
Professora Auxiliar do Departamento de Química da Universidade de Aveiro

Doutor António Augusto Areosa Martins
Investigador de Pós-doutoramento do Laboratório de Engenharia de Processos, Ambiente, Biotecnologia e Energia, Faculdade de Engenharia da Universidade do Porto

Prof. Doutor Carlos Manuel Silva
Professor Auxiliar do Departamento de Química da Universidade de Aveiro

acknowledgments

To Professor Volker Hessel, thank you for all your kindness, thank you for your optimistic advices, and thank you for your support since my first day in the Chemical Reactor Engineering Group.

To Professor Carlos Manuel Silva, thank you for all your support and advice, thank you for always making yourself available in order to help me, and thank you for all your kindness.

To Marc Escribà, first of all, thank you for your friendship. Thank you for all the joy that you spread in the laboratory all day long, and thank you for all your encouragement while we were giving life to this project.

To Dora and Mathew, thank you for your friendships, for all the advices and encouragement, and thank you for always trying to help me seeing the challenges encounter from another perspective.

To Elnaz and Rohit, thank you for your guidance, thank you for your kindness, and thank you for your patience, throughout all the year that I have been in the Chemical Reactor Engineering Group, essentially in my first days working in the laboratory.

To Marlies, Erik, Carlo and Peter, thank you for all your patience, thank you for always making yourselves available to help me in any way possible with any and every kind of challenge encounter during my research project.

To Raquel and Jorge Karam, thank you for all your support, all your advice and criticism, and essentially thank you for your selfless friendship.

To Ana, Joana, Jorge, Michael, Martinique and Patrícia, thank you for your amazing friendship during this long five years.

To my parents, for all their effort, hard work and belief that allowed me to be here today, an enormous thank you.

palavras-chave Anti-solvente, cristalização, escala micro, operação em contínuo,vitamina D_3

resumo

A vitamina D_3 é um micronutriente essencial para o metabolismo do cálcio, sendo esta maioritariamente sintetizada na pele do ser humano, quando exposta a radiação UVB. Contudo, inúmeros factores têm vindo a reduzir a nossa exposição à luz solar, diminuindo assim os níveis de vitamina D_3 no corpo humano a nível global e aumentando a preocupação por parte de diversas instituições médicas a nível mundial. Para superar esta deficiência em vitamina, a vitamina D_3 tem sido adicionada à alimentação humana através de alimentos fortificados e de suplementos alimentares. Para satisfazer a procura da população em vitamina D_3, este trabalho apresenta uma unidade de cristalização com dois estágios que opera em contínuo à escala micro. O objectivo deste trabalho é projectar e optimizar esta unidade de cristalização por forma a desenvolver uma unidade de produção de cristais de vitamina D_3 mais económica, mais sustentável, e com elevado rendimento de cristais aprorriados para aplicações farmacêuticas.

O primiero estágio da unidade de cristalização projetada corresponde a uma coluna de vidro onde a nucleação é intensificada através de cristalização por evaporação e por adição de anti-solvente. Este cristalizador opera a 40 ºC e o caudal volumétrico é controlado manualmente. O segundo estágio é um cristalizador tubular onde a cristalização ocorre por redução da temperatura para promover o crescimento dos núcleos produzidos no estágio anterior. Esta é operada a 7 ºC e em 59 s de tempo de residência. Após o segundo estágio, um filtro está integrado no sistema para recolher os cristais de vitamina D_3 sintetizados.

Este trabalho está dividido em duas partes. A primeira abrange a optimização da unidade de cristalização, a qual foi conseguida estudando o efeito da razão volúmica entre o anti-solvente e o solvente no desempenho da cristalização. O melhor resultado foi obtido para a proporção volúmica de 3, a qual permitiu alcançar 52 % de rendimento absoluto e 60 % de eficiência de filtração. Adicionalmente, por forma a melhorar o rendimento e a eficiência de filtração, ensaios experimentais foram realizados onde a corrente de permeado (da filtração) foi reciclada. Porém, as melhorias esperadas não se verificaram, o que significa que ensaios experimentais adicionais são necessários para sustentar uma conclusão sólida relativamente ao efeito do reciclo no processo em estudo. A reprodutibilidade do processo desenvolvido e optimizado também necessita ser melhorada.

A segunda parte corresponde à caracterização dos cristais de vitamina D_3 produzidos durante os ensaios de optimização. Os cristais apresentam uma forma prismática e aglomeração significativa. A distribuição de tamanhos dos cristais é ampla, extendendo-se desde, aproximadamente, 0.25 µm a quase 500 µm. Adicionalmente, a estrutura dos cristais produzidos não corresponde à estrutura termodinamicamente mais estável. Excluindo o seu hábito, as características dos cristais produzidos não são adequadas para aplicações na indústria farmacêutica. No entanto, sugestões são apresentadas para melhorar ambas as características dos cristais e a optimização do processo.

keywords Anti-solvent, continuous operation, crystallization, microscale, vitamin D_3

abstract

Vitamin D_3 is an essential micronutrient for calcium metabolism, which is mainly synthesized in the skin of the human organism when irradiated with UVB light. However, a variety of factors have been reducing our exposition to sunlight, and thus the levels of vitamin D_3 in the body have been decreasing, rising the concern of numerous medical institutions worldwide. To overcome such vitamin deficiency, the vitamin D_3 has been added to the diet through fortified food and dietary supplements. To address the population demands on vitamin D_3, this project presents a two-stage crystallization unit that operates continuously at a microscale. The aim of this project is to design and optimize this crystallization unit in order to develop an economical and sustainable high yield production unit of vitamin D_3 crystals suitable for subsequent pharmaceutical applications.

The first stage of the designed crystallization unit corresponds to a glass column where nucleation is enhanced by evaporation and anti-solvent crystallization. This crystallizer operates at 40 ºC and the volumetric flow rate is manipulated manually. The second stage is a tubular crystallizer where a cooling crystallization takes place to further grow the nuclei generated in the previous step; it is carried out at 7 ºC and 59 s of residence time. At the end of the second stage, a filter is placed to collect the synthesized vitamin D_3 crystals.

This work is divided in two main parts. The first part comprehends the optimization of the crystallization unit, which was accomplished by studying the influence of the anti-solvent/solvent volumes ratio on the performance of the crystallization. The best results were obtained for the volume ratio of 3, where 52 % of absolute yield was achieved as well as 60 % of filter efficiency. Furthermore, other experiments were performed where the permeate stream (of the filtration) was recycled to improve both yield and filter efficiency. However, such expected improvements were not confirmed, which means that additional experiments are needed to support any reliable conclusion regarding the effect of recycling on the process. The reproducibility of the crystallization process developed and optimized needs to be improved as well.

The second part corresponds to the characterization of the crystals produced during the optimization assays. The crystals exhibit a prismatic habit and a significant degree of agglomeration. The crystal size distribution is large, extending from ca. 0.25 µm to almost 500 µm. Furthermore, the obtained solid-state form is not the thermodynamically stable one. Besides the crystal habit, the properties of the obtained crystals are not yet suitable for a pharmaceutical application. Nonetheless, suggestions of improvement are presented for both crystals characterization and optimization of the crystallization process.

List of Contents

List of Figures

List of Tables

Nomenclature

Abbreviations

CSD	Crystal Size Distribution
DSC	Differential Scanning Calorimetry
ES	Endocrine Society
FDA	Food Drug Administration
IOF	International Osteoporosis Foundation
IOM	Institute of Medicine
MSMPR	Mixed-Suspension Mixed-Product Removal
NMR	Nuclear Magnetic Resonance
PFA	Perfluoroalkoxy
PXRD	Powder X-ray Diffraction
SEM	Scanning Electron Microscopy
UVB	Ultraviolet B

Greek Symbols

γ	Interfacial free energy (J m^{-2})
η_{D_3}	Absolute yield of vitamin D_3 (%)
$\eta_{D_3,corrected}$	"Corrected" absolute yield of vitamin D_3 (%)
θ	Wetting angle (º)
μ_{liquid}	Chemical potential of the solute in solution (J mol^{-1})
$\mu_{liquid,eq}$	Chemical potential of the solute in solution at the equilibrium (J mol^{-1})
μ_{solid}	Chemical potential of the solute as solid phase (J mol^{-1})

σ	Relative supersaturation
τ	Residence time (s)
$\Delta\mu$	Chemical potential difference (J molecule^{-1})
$\Delta G_{nucleus}$	Gibbs free energy of a nucleus (J)
$\Delta G_{surface}$	Gibbs free energy of cluster's surface (J)
ΔG_{volume}	Gibbs free energy of cluster's volume (J)
$\Delta G_{heterogeneous}$	Gibbs free energy of a nucleus in heterogeneous primary nucleation (J)
$\Delta G_{homogeneous}$	Gibbs free energy of a nucleus in homogeneous primary nucleation (J)

Symbols

c_m	Metastable limit
$c_{p,m}$	Molar heat capacity at constant pressure (J mol^{-1} K^{-1})
c_s	Solubility curve
d_{50}	Mean particle diameter (μm)
d_i	Internal diameter of the tubular crystallizer (mm)
k_a	Surface shape factor
k_v	Volume shape factor
m_{D_3}	Mass of vitamin D_3 (mg)
m_{feed}	Mass of vitamin D_3 in the feed (mg)
m_{filter}	Mass of vitamin D_3 collected in the filter (mg)
$m_{filter,1}$	Mass of vitamin D_3 collected in the filter during Cycle 1 (mg)
$m_{filter,2}$	Mass of vitamin D_3 collected in the filter during Cycle 2 (mg)
m_{max}	Maximum mass of vitamin D_3 that can crystallize (mg)
$m_{permeate}$	Mass of vitamin D_3 in the permeate stream (mg)
$m_{permeate,2}$	Mass of vitamin D_3 in the permeate stream obtained from Cycle 2 (mg)
m_{pumped}	Mass of vitamin D_3 pumped to the system (mg)
$m_{pumped,t}$	Total mass of vitamin D_3 pumped to the system (mg)
n_{D_3}	Molar quantity of vitamin D_3 (mole)
r^*	Critical cluster radius (m)

x	Temperature of the solution (ºC)
y	Concentration of vitamin D_3 in the solution (mmol L^{-1})
C_{D_3}	Molar concentration of vitamin D_3 (mol L^{-1})
$Filter\ eff.$	Filter efficiency (%)
G	Gibbs free energy of formation (J)
H	Enthalpy (J)
H^0	Enthalpy at 0 K (J)
M_{D_3}	Molar mass of vitamin D_3 (g mol^{-1})
L	Size of the cluster (m)
L_t	Length of the tubular crystallizer (mm)
Q_v	Volumetric flow rate (mL h^{-1})
S	Entropy (J K^{-1})
S^0	Entropy at 0 K (J K^{-1})
S_{D_3}	Solubility of vitamin D_3 in acetonitrile (mg mL^{-1})
T	Absolute temperature (K)
V	Volume of the tubular crystallizer (mL)
V_{AS}	Volume of the anti-solvent (mL)
V_m	Molar volume (m^3 $molecule^{-1}$)
$V_{solvent}$	Volume of the solvent (mL)

Chapter 1

INTRODUCTION

Start where you are. Use what you have. Do what you can.
Arthur Ashe

This chapter introduces the theoretical background of this research and contextualizes the problem of this research work. Furthermore, it presents the objectives of this research as well as the structure of the thesis.

1.1. Vitamin D

Vitamins are nutrients needed in small doses and are not produced by the organism of a human being. Therefore, they need to be obtained through the diet. [1] Vitamin D is a fat-soluble steroid that comprises a group of molecules called calciferols. The most addressed calciferols for the human body are ergocalciferol and cholecalciferol, commonly known as Vitamin D_2 and Vitamin D_3, respectively. [2]

Vitamin D_3 is mainly obtained through a photochemical reaction induced by the sunlight adsorbed in the skin. The compound 7-dehydrocholesterol, present in the basal and suprabasal layers of the epidermis, when exposed to ultraviolet B radiation, UVB, produces previtamin D_3. The later undergoes a process that includes thermal isomerization from which vitamin D_3 is produced. Vitamin D_3 is not biologically active until enzymes functionalize it. Therefore, in the liver, vitamin D_3 will be transformed in 25-hydroxycholecalciferol, also called 25-hydroxyvitamin D_3. Further hydroxylation in the kidney will convert 25-hydroxycholecalciferol into 1,25-dihydroxycholecalciferol (see Figure 1.1). This compound is an endogenous hormone that regulates the calcium uptake in the intestines and the calcium levels in the bones and kidney. [1] [2]

Vitamin D_2 is a plant-derived micronutrient which is produced in a similar way of vitamin D_3. Moreover, vitamin D_2 is also converted into a hormone named as 1,25-hydroxyergocalciferol, or 1,25-hydroxyvitamin D_2. Both vitamins possess similar chemical structure and biological action.

However, vitamin D_3 has been reported in many studies to be superior to vitamin D_2 due to its higher bioavailability. [2]

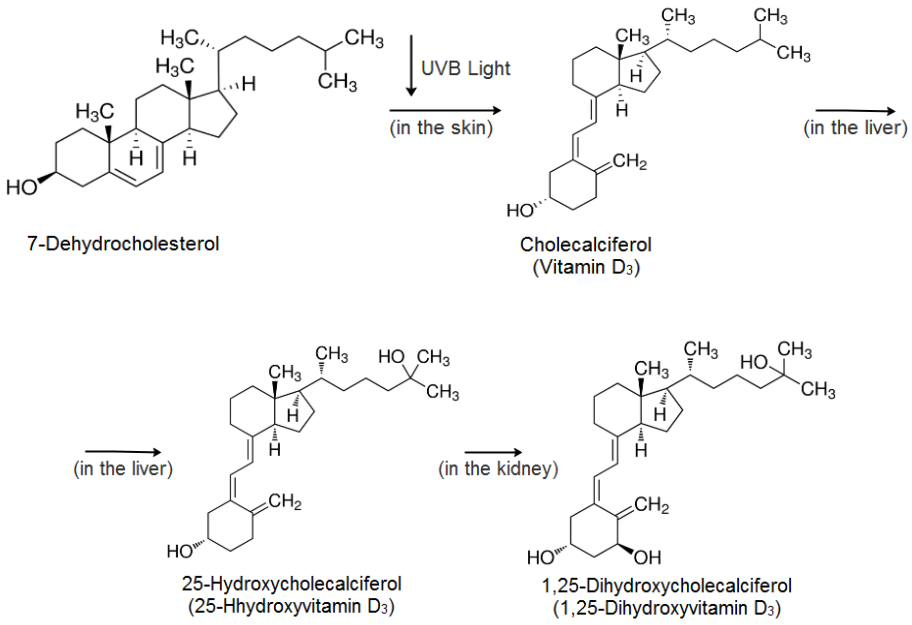

Figure 1.1 Scheme of vitamin D_3 production in the skin and further transformation into the endogenous hormone 1,25-dihydrocholecalciferol. [1]

Besides its synthesis in the human body, vitamin D_3 can also be obtained by the diet. The main naturally produced dietary sources of Vitamin D_3 are animal food products. Examples are fat fishes and fish liver oils, which have the highest content in Vitamin D_3 (see Table 1.1). Vitamin D_2 has the highest content in wild grown mushrooms. However, the most commercialized mushrooms, the white button mushroom, have a very low level of that vitamin (see Table 1.1). Some producers even irradiate those mushrooms with UVB light to increase its content in vitamin D_2. Vitamin D can also be found in eggs and in dairy products, such as cheese and butter. [2]

Both healthy diet and daily exposition to sunlight are necessary to reach the daily levels of vitamin D required by the human body. The vitamin D status of a human being can be evaluated by measuring the serum concentration of 25-hydroxyvitamin D. This substance is the main circulating form of vitamin D and it is used as a biomarker because it reflects the dietary intake of both vitamin D_2 and D_3, and the production of the endogenous hormone from vitamin D_3. [2] Lips and his colleagues have defined four different levels for the concentration of 25-hydroxyvitamin D in the human's blood (see Table 1.2). [3] Different institutions did not agree with the classification of 50 nmol L^{-1} as repletion level. The Institute of Medicine, IOM, has stated that 50 nmol L^{-1} should be defined as the concentration at which 97,5 % of the vitamin D in need would be covered. On the

other hand, the Endocrine Society, ES, has stated that the repletion level should start at 75 nmol L^{-1} rather than 50 nmol L^{-1}. [2]

Table 1.1 Vitamin D content of different food products. [2]

		Range
		μg Vitamin D per 100 g
Raw products		
Fish	Salmon	4.2 – 34.5
	Perch	0.3 – 25.2
	Tuna	1.7 – 18.7
	Cod	0.5 – 6.9
Mushrooms	Wild grown mushrooms	0.3 – 29.8
	White bottom mushrooms	0 – 0.2
Animal products	Pork meat	0.1 – 0.7
	Chicken meat	0 – 0.3
	Beef Liver	0 – 14.1
	Eggs	0.4 – 12.1
Processed foods		
Fish	Tuna liver oil	144,400
	Cod liver oil	137.5 – 575.0
	Canned sardines	3.2 - 10
Mushrooms	Irradiated Mushrooms	6.6 – 77.4
Dairy products	Butter	0.2 – 2.0
	Cheese	0 – 0.1

Table 1.2 Classification of the concentration of 25-hydroxyvitamin D in the human's blood. [3]

Concentration (nmol L^{-1})	**Classification**
< 12.5	Severe deficiency
12.5 – 25	Deficiency
25 – 50	Insufficiency
>50	Repletion

The importance of keeping the levels of vitamin D superior to 75 nmol L^{-1} is essential for the bone metabolism. This vitamin is a key for a healthy bone development and reduces the risk of bone diseases like osteoporosis and rickets. [2] Furthermore, Grant and colleagues have reported the

benefits of vitamin D, well supported by research, in reducing the risk of many other diseases, such as cardiovascular diseases and cancer [4] (see Figure 1.2).

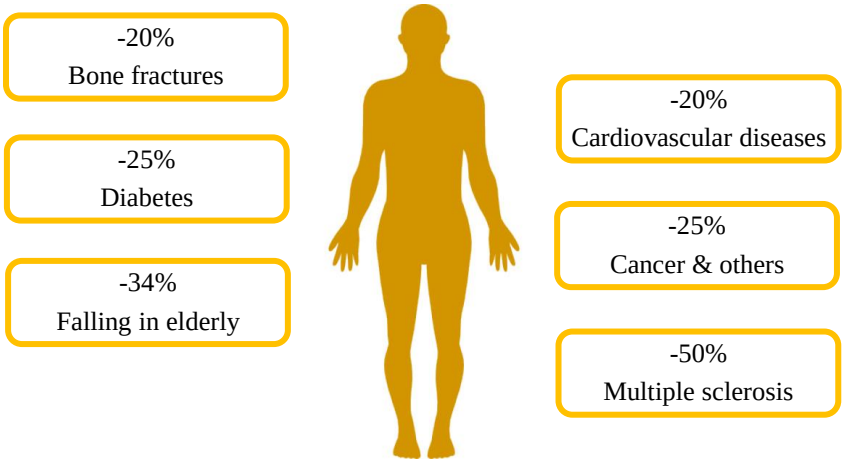

Figure 1.2 Benefits of optimal levels of Vitamin D for the human being. [4]

As a consequence of the dimension in the human body of the vitamin D impact, this compound can additionally improve the health economics of a country. Grant determined that a rise of 40 nmol L^{-1} in vitamin D levels would help save up to 16.7 % of health care costs. [4]

1.2. Deficiency of Vitamin D_3

Many organizations have identified vitamin D deficiency or insufficiency as a public health problem that has grown worldwide. [2] In fact, the International Osteoporosis Foundation, IOF, has developed a global vitamin D map to expose this problem. This map is a result of an extensive review of worldwide 25-hydroxyvitamin D plasma levels available in reliable published publications. In 2014, from an analysis of this map, Hilger has shown that 6.7 % of the overall population presented 25-hydroxyvitamin D levels below 25 nmol L^{-1}, 37.3 % below 50 nmol L^{-1} and only 11.9 % of the population exhibited levels above 75 nmol L^{-1}. [2] [5]

Many reasons can be associated to this worldwide vitamin D deficiency. To begin with, malnutrition, a condition where the diet does not match to provide the adequate level of vitamin D. Furthermore, the level of this vitamin is also dependent on the solar UVB radiation that reaches the skin. This changes with geographic latitude, season of the year and time of the day. Currently, other factors help reducing the exposition of the skin to sunlight. Those are severe air pollution in large cities, less outdoor activity as a consequence of an unhealthy life style change, and topical application of sunscreen with high sun protection factors. [2] The latter is a result of the intense solar radiation that can promote skin cancer, among other diseases. Consequently, exposition to sunlight must be moderated but regular to promote vitamin D synthesis. [2] [6] The immobility of elderly population

compromises their vitamin D levels as well as the decline of 7-dehydrocholesterol characteristic of aging. [2]

As the main source of vitamin D, more specifically vitamin D_3, is being compromised, there is a need to improve vitamin D status worldwide by food fortification, or dietary supplements. Some countries have already taken measures to adjust the national recommendations for dietary intake of vitamin D. For example, the United States increased the daily intake for children since the first days of life. In 2008, the American Academy of Pediatrics increased the level for 400 IU and in 2010 the IOM increased it for 600 IU. In 2012, medical organizations from Germany, Austria and Switzerland also increased the recommended daily vitamin D intake to 800 IU for all age groups starting from 1 year of age. [2] Currently, Finland has already eradicated vitamin D deficiency due to mandatory food fortification. The first targets were children and adolescents by increasing the content of vitamin D in most milks, sour milks and yogurts. [7]

1.3. Industrial production of Vitamin D_3

To accomplish the goals established by different countries and to overcome the deficiency of vitamin D, this compound needs to be produced industrially as a pure crystalline vitamin. Currently, it is difficult to know how is being developed the production of vitamin D_3 due to the competitive nature of the market. [8] Nevertheless, it has been found a process diagram of vitamin D_3 manufacture process, dated from 1999 (see Figure 1.3). [9]

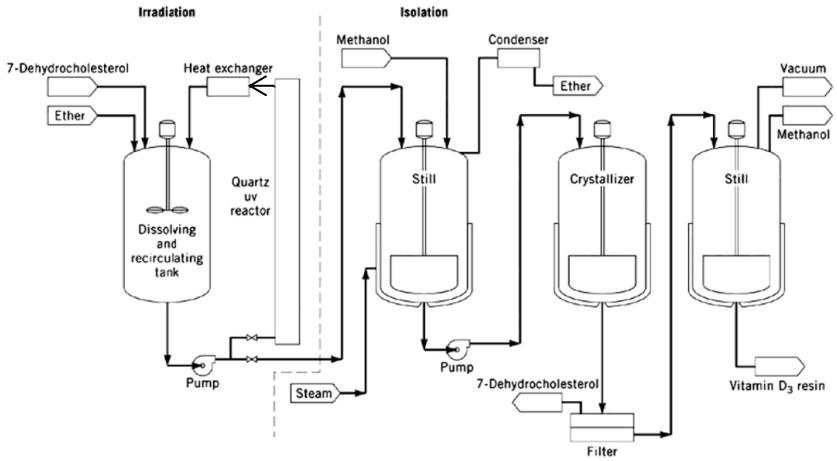

Figure 1.3 Flow diagram of the manufacturing process of vitamin D_3. [9]

As it can be seen, there are two stages in the production of the vitamin D_3, reaction stage and isolation stage. During the first one, 7-dehydrocholesterol is dissolved in an appropriate solvent, such as free peroxide diethyl ether, and then pumped to a UV-transparent reactor where the photochemical reaction is promoted. The second stage starts with the evaporation of the solvent of the outlet stream.

The latter is made of unconverted reactant, pre-vitamin D_3, vitamin D_3 and irradiation by-products. While the ether is being removed, another solvent is added to the mixture to promote the crystallization of the reactant in the next vessel. After the crystallization, that solvent is removed also by evaporation obtaining at the end vitamin D_3 in a resin form. [9] This resin form is mainly used for supplementation of animal feeds. Concerning vitamin D_3 for human consumption, in 2012, there was still no crystalline vitamin D_3 form that was approved by U.S Food Drug Administration, FDA. [8] The separation and purification of vitamin D_3 is quite difficult. The resin is often subject to an expansive low yield chemical complexation. [9]

Despite these challenges reported from 1999, the vitamin D_3 market is expected to reach $2.5 Billion by 2020. [10] The key players in this market, such as Nestlé S.A. (Switzerland), Koninklijke DSM N.V. (The Netherlands), among others, are focusing on the expansion of their facilities and investing in R&D activities to gain a competitive edge through new product developments. [10]

1.4. Objectives of the Thesis

The project named "Microprocessing photovitamin D_3 using photo-high-temperature intensification" has been developed to satisfy the worldwide need of pure crystalline vitamin D_3 suitable for pharmaceutical and food applications. That project aims to design an economical and sustainable high yield production unit for vitamin D_3. The production unit under development is divided in three operation steps: synthesis of vitamin D_3, purification of the synthesis outlet stream and vitamin D_3 crystallization.

The work of this thesis is related with the last step of the unit, the vitamin D_3 crystallization. This study aims to optimize the crystallization process through a microscale continuous flow operation, which enhances mass and heat transfer, and process control, as well as increases material throughput in lower residence time. Furthermore, this project aims to characterize the vitamin D_3 crystals synthesized in order to assess their applicability in pharmaceutical industry.

1.5. Outline of the Thesis

This thesis is organized in four parts. The first part, which corresponds to the second chapter, is a literature review where it is described the phenomenon of crystallization, are presented the advantages of a continuous crystallization in a sub-millimeter scale and is approached the characterization of crystals. Furthermore, there is a chapter where one describes the methods applied to achieve the goals of this thesis. The forth chapter is a sequence of the previous one, where the results are presented and discussed. Last but not the least, there is a chapter dedicated to the conclusions of this report where are highlighted the possible improvements in this study.

Chapter 2

LITERATURE REVIEW

Nothing in life is to be feared, it is only to be understood.
Now is the time to understand more, so that we may fear less.
Marie Curie

The study developed is essentially based on the separation technique of crystallization. Therefore, this chapter initially presents a literature survey to clarify the fundamentals behind a crystallization phenomenon. This chapter will start with a general approach of crystallization and will grow further in crystallization from solution. Furthermore, this review will present a subchapter where it is discussed the operation mode of crystallization, continuous operation at a micro scale.

2.1. Crystallization

Crystallization is one of the oldest separation processes known by mankind. As an example, crystallization is the method responsible for the collection of sodium chloride crystals via evaporation of seawater. Scientifically crystallization is defined as "*the phase transformation of a compound from a fluid or an amorphous solid state to a crystalline solid state"*. [11] The *crystalline solid state*, also known as crystal, is ideally a pure three-dimensional ordered structure. The latter is stablished by forces at the molecular level actuating during crystallization. [12]

Crystallization is based on a phase change of at least one of the compounds of a mixture. Therefore, the phase diagram of the mixture is an important tool to better understand and operate the system. Depending on the phase diagram, different crystallization methods can be applied (see Figure 2.1). [11] [13] For example, Figure 2.1(c) describes the thermodynamic behavior of a compound easily crystallized from an inert gas phase without going through a liquid phase. That method is called crystallization from a vapor or desublimation. Melt crystallization is a method mostly applied to eutectic-forming systems (see Figure 2.1(b)). Eutectic is the composition of a binary liquid mixture where both compounds solidify at a specific temperature. Under that temperature, the compounds

are theoretically obtained as pure solids. Melt is the name given to a eutectic-forming system as a homogeneous liquid phase. [14] Melt crystallization is mainly used as a purification operation due to high purity values achieved within this process, values close to 99.9 %. Figure 2.1(a) presents solubility curves of different compounds in an aqueous system. That phase diagram is the most suitable for the method called crystallization from solution. When this process is applied, highly pure crystals can be produce in a single crystallization stage, unlike melt crystallization. [13]

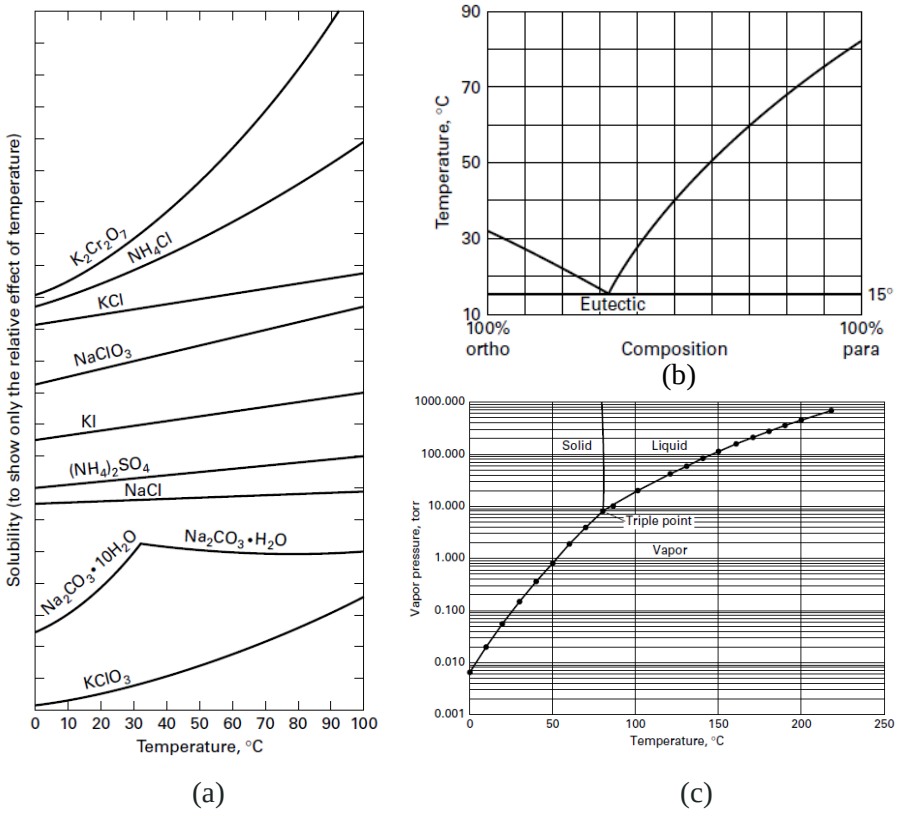

Figure 2.1 Phase diagrams characteristic of different crystallization systems: (a) Solubility curves of diverse aqueous systems suitable for crystallization from solution; (b) Eutectic-forming system of ortho- and para-chloronitrobenzene suitable for melt crystallization; (c) Phase diagram of naphthalene, a compound suitable for vapor crystallization. [14]

2.1.1. Crystallization from solution

Figure 2.2. presents a solubility curve, c_s. As mentioned in the previous section, that phase diagram is the most suitable for crystallization from solution. A solution is a homogeneous phase mixture of two or more compounds. The most abundant compound is generally called solvent and the remaining are called solutes. For a temperature T_1, when the solute concentration in the solution is equal to point a (see Figure 2.2), the solution is said to be undersaturated. In this condition, the

solid phase is always dissolved in the solvent, and the solution is always homogeneous. [13] [14] [15]

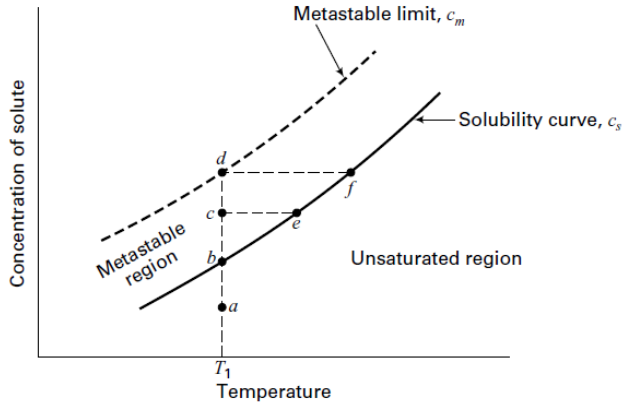

Figure 2.2 Representation of a crystallization from solution phase diagram where both solubility curve, c_s, and metastable limit, c_m, are presented. [14]

If the concentration of the solute increases until point b, the chemical potential of the solute in solution, $\mu_{liquid,eq}$, will be equal to the chemical potential of the solute as solid phase, μ_{solid}. Therefore, the solution is in equilibrium with the solid phase of one of the solutes. In this condition, the solution is called saturated with respect to that solid phase, and the concentration of that solid phase is its solubility. [13]

The solubility of a solute is dependent on the temperature of the solution, and that dependency is described by the solubility curve (see Figure 2.1 and 2.2). [15] The concentrations of point e and f are solubility values as well. However, they are solubility's of the same solute for distinct temperatures. Figure 2.2 presents a solubility curve, c_s, that, like most of the systems, describes a system where the solubility of the solute increases when temperature increase. [14] [15]

If the concentration of the solute further increases, point c, a solid phase starts to appear in the system. In this situation, the solution is said to be supersaturated with respect to the dissolved solute, and the chemical potential of the solute in solution, μ_{liquid}, is now higher than the corresponding equilibrium value. The difference between the chemical potential of the solute in the supersaturated and the saturated states (see equation 2.1) is called supersaturation degree.

$$\Delta\mu = \mu_{liquid} - \mu_{liquid,eq} = \mu_{liquid} - \mu_{solid} \quad (2.1)$$

The supersaturation degree is a prerequisite for crystallization and it is denominated as the driving force of the crystallization process. [15] The degree of supersaturation at point c is related with the concentration difference between points b and c. [14]

Further increase in solute's concentration will increase the degree of supersaturation until it achieves the supersaturation limit, point d. That limit is also known as metastable limit, c_m. In the metastable region, a small amount of solute entities is formed and is stable in the solution which behaves like a suspension. At the metastable limit a reasonable amount of solid phase is formed and the crystallization spontaneously takes place. [13] [14]

The decrease of temperature can also supersaturate a solution. For example, from points f to d, the decrease in temperature decreases the solubility of the solute. Therefore, new solid phase appears driving the solution into the metastable region. From point e to c the same phenomenon is verified. Nevertheless, the decrease in temperature is still not enough for the solution to achieve the metastable limit and spontaneously crystallize. [14] [15]

The crystallization phenomenon starts with the development of crystals' nuclei, step called nucleation. This step is followed by further development and growth of the nuclei until the final crystalline structure is obtained, step called crystal growth. Nucleation and crystal growth are the two dominant rate processes that characterizes crystallization from solution. The manipulation of these mechanisms influences most of the final properties of the produced crystals, such as number, crystal size distribution and habit. [13]

2.1.1.1. Nucleation

Nuclei can be obtained by solute entities that spontaneously start clustering together. In this specific case, nucleation is called homogeneous primary nucleation. However, in practice the primary nucleation phenomenon is mostly heterogeneous, i.e., spontaneous nucleation occurs in the presence of foreign particles in solution, such as dust or dirt. Moreover, nucleation can also be promoted by crystals of the crystallizing compound that are already present in the solution. In that situation, nucleation is called secondary nucleation. [13] [15]

2.1.1.2. Homogeneous Primary Nucleation

Primary nucleation, accordingly with the Classical Nucleation Theory, starts with the formation of clusters. These clusters are a result of the attachment and detachment of solute entities in the solution. In an undersaturated or just saturated solution, the formation and decay of clusters is in equilibrium and the solution is stable against new phase formation. When the solution reaches a supersaturation state, clusters of a critical size are formed that either fall apart or became nuclei that grow further. [13]

Thermodynamically, the attention falls into the Gibbs free energy of a nucleus, $\Delta G_{nucleus}$. This is characterized by two energy terms, defined in equations 2.2 and 2.3 [13], and it has to verify the condition described by equation 2.4 for nucleation to occur [13] [16]:

$$\Delta G_{nucleus} = \Delta G_{volume} + \Delta G_{surface} \tag{2.2}$$

$$\Delta G_{nucleus} = -\frac{k_v L^3}{V_m}\Delta\mu + k_a L^2 \gamma \tag{2.3}$$

$$\Delta G_{nucleus} < 0 \tag{2.4}$$

where k_v and k_a are volume and surface shape factors, L is the characteristic length, V_m is the molecular volume, $\Delta\mu$ is the chemical potential difference per solute molecule in the fluid and the solid, and γ is the interfacial free energy.

The first term, ΔG_{volume}, defines the energy variation due to the addition of a solute entity into a cluster, which is negative in a supersaturated solution. The second term, $\Delta G_{surface}$, defines the energy variation associated with the surface increment of the cluster surface. This free energy term is positive, since the interfacial tension between nucleus and solvent is positive. [11] [13]

Figure 2.3 describes the behavior of the Gibbs free energy of a nucleus as the size of a cluster increases, assuming that a cluster has a sphere shape. As it can be seen, $\Delta G_{nucleus}$ achieves a maximum value for a specific radius, r^*, which is the energy barrier that the system needs to overcome for nucleation to happen. For a radius below r^*, the $\Delta G_{nucleus}$ is positive and increases with increasing radius. [11] [13] A positive Gibbs free energy indicates that growth of a cluster is unfavorable, thus the system is not stable. Therefore, the clustering of solute entities below that critical size tend to decay in order to reduce the Gibbs free energy. When the cluster size is equal to r^*, the probability of adding or losing a solute entity is equal. The cluster is said to be in equilibrium with the supersaturated solution. As soon as the cluster has a radius superior to the critical value, the $\Delta G_{nucleus}$ starts decreasing. The nucleus will continue to grow since attachment of solute entities reduces Gibbs free energy increasing the stability of the nucleus. Therefore, the nucleation will proceed spontaneously. [13] [16]

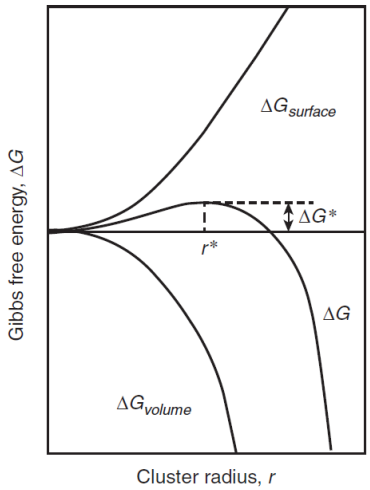

Figure 2.3 The Gibbs free energy, ΔG , as a function of the radius, r, of a cluster. [13]

The change in number of critical clusters within a certain time in a certain volume is defined as nucleation rate. [13] This rate is dependent on the degree of supersaturation of the system. For a small supersaturation degree, the system does not have enough energy for nucleation, and thus the nucleation rate will be also very small, practically zero. As the supersaturation degree of the system increases, the nucleation rate deviates considerably from zero. From that stage on, any supersaturation increment will rise the nucleation rate dramatically. Moreover, it is possible to notice nucleation at a macroscopic level. [11] [13]

2.1.1.3. Metastable limit

As mentioned before, the metastable zone is a region where the system is supersaturated. However, the solid phase already formed is stable in solution without spontaneously nucleating. [11] [15] The boundaries of this metastable zone are the solubility curve of the system and a theoretical line named metastable limit (see Figure 2.2). Above this limit is the labile zone where the system is still supersaturated but nucleation occurs spontaneously. [15]

The degree of supersaturation needed for spontaneous nucleation will define the width of the metastable zone. However, the experimental conditions and the characteristics of the system can also influence the metastable zone width. [11] [13]

2.1.1.4. Heterogeneous Primary Nucleation

Primary nucleation can also occur in the presence of foreign particles, which will spontaneously induce nucleation in their surface decreasing the associated Gibbs free energy. [11] The Gibbs free energy of nucleation in a surface, $\Delta G_{heterogeneous}$, can be related with the Gibbs free energy of homogeneous nucleation, $\Delta G_{homogeneous}$, by a factor φ (see equation 2.5). Comparing the solute as solid phase with a droplet and assuming that the particle's surface is flat, this factor is related with the wetting of the particle surface by a droplet which is characterized by the contact angle between the two interfaces, θ. This angle indicates whether the presence of the substrate will substantially lower the nucleation barrier. The angle range is between 0 º and 180 º. For a $\theta = 180$ °, $\varphi = 1$. For this situation, the droplet will not spread on the surface because is energetically not favorable. Therefore, the foreign particles do not support nucleation. On the other hand, for complete wetting, $\theta = 0$ °, $\varphi = 0$. In this case, the droplet spreads on the surface and there is no energy barrier to overcome for nucleation to occur.

$$\Delta G_{heterogeneous} = \varphi \Delta G_{homogeneous} \tag{2.5}$$

The factor φ is always smaller than 1. Therefore, the heterogeneous nucleation will be always more energetically favorable than the homogeneous one. Moreover, the nucleation rates will be higher even for a lower degree of supersaturation. Attention needs to be given to this energy reduction in order to avoid the presence of impurities in the final crystals. [11] [13]

2.1.1.5. Secondary Nucleation

Crystals of the solute can exist in solution since the beginning of the process. Their presence will induce nucleation for a very low degree of supersaturation. This phenomenon is called secondary nucleation. There are a variety of mechanisms to promote secondary nucleation, but the most relevant is attrition breeding. In this method, the larger crystals collide with the impeller and the walls of the crystallizer and with other crystals becoming smaller crystals that act as nuclei. [13]

2.1.1.6. Crystal growth

In a supersaturated system, some solute entities will add to the nucleus produced through a 2-dimensional molecular self-assembling promoting the growth of the nucleus into the final crystals. This rate process is defined as crystal growth. The mechanism of crystal growth starts with the migration of solute molecules from the bulk solution to the nucleus surface. These molecules are adsorbed and then diffuse on the surface until they find a suitable site to integrate the crystal lattice. [14] [17] The conditions for crystal growth are optimal when the system is at the metastable zone. [18]

2.1.2. Methods of Crystallization from solution

Crystallization from solution can be operated in four different methods: cooling of the solution, evaporation of the solvent, precipitation by addition of a reactant and addition of an anti-solvent. The initial step to select the most suitable method for a specific system is by analyzing the solubility curve of the system. [13]

2.1.2.1. Cooling of the solution

In cooling crystallization, the supersaturation of a solution is promoted by decreasing the temperature (see Figure 2.4). This decrease will reduce the solubility of the solute promoting a mass transfer of the solid from the solution to the solid phase. As the solubility decreases more solute entities are in suspension supersaturating the solution. Further decrease of the temperature will start nucleation thus will start the formation of crystals. [11] [13]

Cooling crystallization is mostly applied for moderate to highly soluble solutes whose slope of solubility curve is positive and steep, i.e., slope usually higher than $0.005^{o}C^{-1}$. The feed and the

crystallizer temperatures are usually lying in the temperature range of the steepest region of the solubility curve. Therefore, a reasonable large amount of solid is obtained for a small temperature range. [13]

The crystallizer temperature needs to be as low as possible to minimize the product loss. However, the yield of the crystallization will be restricted by the solubility of the solid at the lowest temperature of the process. This limitation is the main obstacle of cooling crystallization which can be overcome by recycling the solution upstream in the process. Otherwise the solution will be conducted to a second crystallization step like anti-solvent crystallization. [13]

From an energy point of view, cooling crystallization is the best option and is a simple operation. In stirred crystallizers, heat exchange can occur by indirect and direct cooling. Indirect cooling occurs via the scrapped or non-scrapped surface of the crystallizer. For systems with intense scale, direct cooling is a better option which is promoted by adding an immiscible liquid or gas, called refrigerant, into the solution. Vacuum cooling, also known as vacuum crystallization or flash cooling crystallization, can also be an option for intense scaled systems. The pressure in the crystallizer is kept below the vapor pressure of the solution. Therefore, the solvent flashes off and the solution is adiabatically cooled down until the boiling temperature of the solution for the crystallizer's pressure. This operation is applied, for example, in multi-stage operation and in vapor recompression decreasing the energy consumption. [13]

2.1.2.2. Evaporative crystallization

Evaporative crystallization is a concentration-driven method promoted by decreasing the quantity of the solvent. The latter will rise the concentration of the solute in the solution supersaturating the system (see Figure 2.4). Further removal of the solvent will promote nucleation initiating crystals formation. [11]

Similarly, to cooling crystallization, evaporative crystallization is mostly used for moderately to highly soluble compounds. The solubility curve of the systems that undergo this crystallization method has a flat slope because cooling crystallization results in a low yield for those systems. However, evaporative crystallization can be applied regardless the solubility curve's slope of the system. [13]

The majority of the evaporative systems are operated at high temperature, above 50 ºC, and use low pressure steam, 4 bar, or by-product steam, 1 to 2 bar, from another chemical process. This crystallization method, as well as cooling crystallization, is not suitable for thermally unstable compounds and solid solutions. [13]

The energy consumption of this method is higher than the cooling crystallization. In continuous evaporative crystallization, in order to reduce the energy demand, multiple-effect

evaporation is applied. In this operation, the heat needed to vaporize the solvent in an effect is provided by the condensation of the solvent from a previous effect. Another option is a single effect evaporator with mechanical or thermal vapor recompression. These evaporators are denominated reduce-pressure evaporative crystallizers to distinguish them from vacuum cooling, which operates without an external heat source. Nevertheless, vacuum evaporation is often selected in order to take advantage of cooling and evaporation simultaneously. [13]

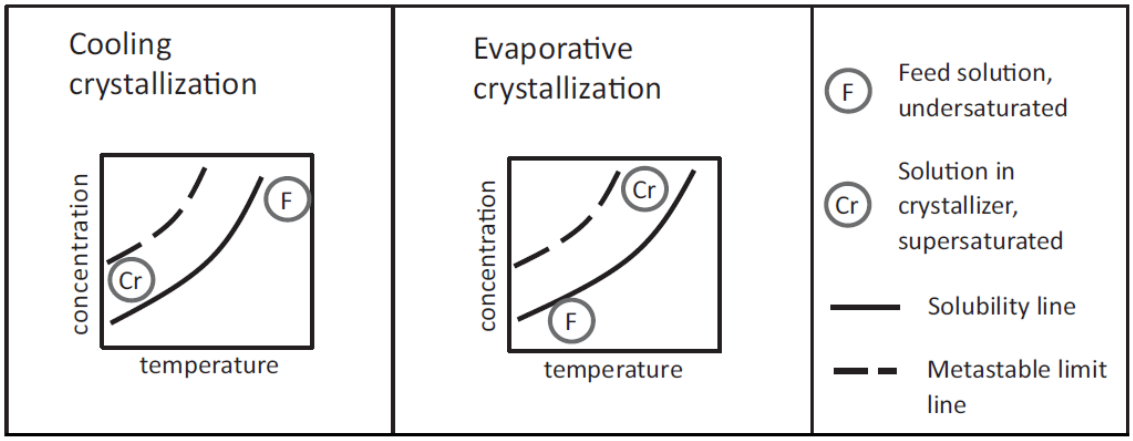

Figure 2.4 Scheme of the cooling and evaporative crystallization through a solubility curve. [13]

2.1.2.3. Precipitation [13] [14]

Precipitation is applied for substances whose solubility in a specific solution is very low. This method is mainly based in mixing two miscible reactant streams which will produce a solid compound sparingly soluble in the reaction mixture. If the reactant streams are highly concentrated, the solubility of the product will be largely exceed promoting a fast formation of the solid phase. [13] As a consequence of the high rate of nucleation, specifically primary nucleation, the crystals obtained will be small and are mostly aggregates and agglomerates. [14]

Precipitation promotes the deposition of impurities, such as polymorphs or amorphous materials, together with the product and a high agglomeration rate. In order to improve the quality of the solid phase, measures should be taken to reduce the supersaturation degree at the inlet of the crystallizer, such as decreasing the mixing time. [13]

2.1.2.4. Anti-solvent crystallization [13]

Anti-solvent crystallization is often coupled to a cooling crystallization step to recover the residual amount of a high added-value product due to the resulting high yields. The method is also suitable for heat sensitive substances that cannot undergo an evaporative or cooling crystallization.

An anti-solvent is usually a liquid added to a solution in order to decrease the solubility of the solute in the mixture. The solubility reduction will depend on the ratio between the solvent and the anti-solvent abundancies. The addition of the anti-solvent also dilutes the mixture. Therefore, crystallization occurs if the effect of the decrease in solubility is higher than the dilution effect. For an aqueous solution, it is often used an organic liquid as anti-solvent. This will decrease the water activity decreasing the solubility of the solute in the mixture. Sometimes a highly soluble salt is added to the aqueous solution instead of a liquid. This method, called salting out, has the same result as the addition of the organic liquid. The presence of the salt decreases the water activity, thus the solubility of the solute decreases.

The solubility of the solute in this crystallization method is mostly very low which results in a large degree of supersaturation. As a consequence, the crystallization will be fast and the quality of the product will be low, similar to precipitation.

One of the disadvantages of this process is the need to separate the anti-solvent from the remaining mixture.

Figure 2.5 helps understanding how crystallization is promoted in the last two crystallization methods approached, as well as exhibits their similarity.

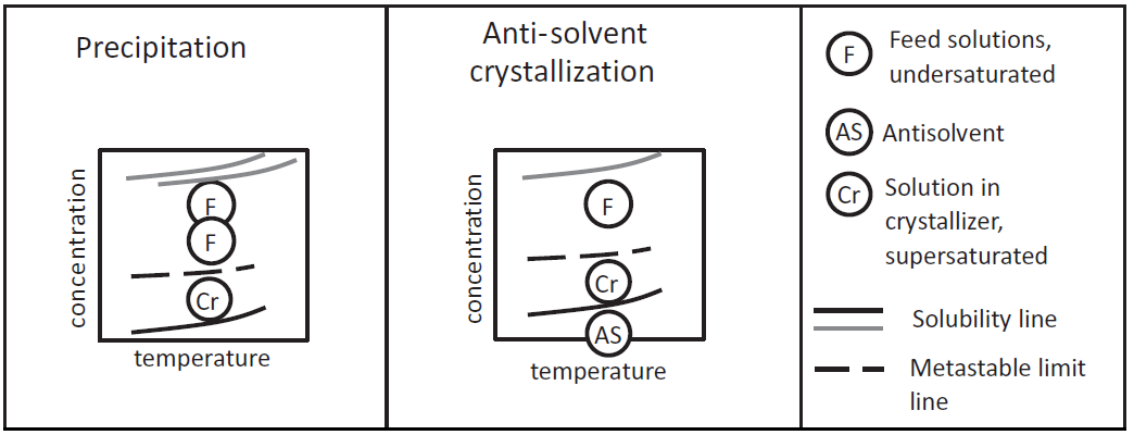

Figure 2.5 Scheme of precipitation and anti-solvent crystallization through a solubility curve. [13]

2.1.2.5. Selection of the crystallization method [13]

The most suitable crystallization method for a specific system is initially chosen based on thermodynamic considerations, which take into account the solubility curve of the solution. Nevertheless, the final decision also depends on operational features of the crystallizing system, such as scaling and thermal stability, economical factors, such as energy consumption, among others.

The specifications of the final crystalline product also influence the selection of the method (see Table 2.1). For a highly pure crystal, melt crystallization is the most suitable method, rather than

crystallization from solution. If the target is large pure crystals, cooling or evaporative crystallization are the best option. Otherwise, for fine solids or agglomerate particles, anti-solvent crystallization and precipitation are the most appropriate.

Table 2.1 Characteristics of the solid product obtained by melt crystallization and the different methods of crystallization from solution. [13]

Crystallization Method	Features of the process		Product quality	
	Solubility (wt %)	Relative supersaturation, σ	Particle size (μm)	Purity
Melting Crystallization	90	0.001 to 0.01	Product is a liquid	Very good
Cooling Evaporative	10 to 30	0.001 to 0.01	100 – 1000	Good
Precipitation Anti-solvent	<0.01	1 to 100	0.5 – 100 (agglomerates)	Poor

2.1.3. Continuous crystallization. Microfluidics crystallization

A crystallization unit is mostly integrated in downstream processing operations as a separation or a purification step. [15] Crystallization can be operated in two different modes, continuously or batch-wise.

Batch operation is mostly applied for multi-purpose units, for processing high-value products due to reduced off-spec losses, and for small production capacities. Although this operation mode is characterized by its simplicity of equipment, it is only an economical option for capacities inferior to 1 m^3day^{-1}. A batch operation provides the possibility of cleaning the crystallizer after every cycle which allows the removal of any encrusted compound, avoiding product contamination and slow formation of undesirable polymorphs. [15]

Although batch crystallizers are the most applied ones, they have limitations, such as low reproducibility and wide size distribution, that compromise the quality of the crystalline product. [12] On the other hand, continuous plug flow crystallizers allow a narrow size distribution and high reproducibility due to the crystallization of the solute under uniform conditions when steady state is achieved. Additionally, the uniform product quality obtained in this operation eliminates the need of downstream corrective actions adopted in batch operation. [12] [19] A continuous crystallizer also benefits from higher productivity and material throughput as well as better process control. The latter allows the control of important product characteristics, such as crystal size distribution. [12]

Microfluidics crystallization

Currently, it is increasing the interest of performing continuous crystallization in a microfluidic system. The microfluidic technology is a tool that provides a better insight of the crystallization phenomenon and crystals formation as well as a better control and manipulation of nucleation and crystal growth. These advantages are applicable for organic, inorganic and metal-organic solid materials. [17] [20]

Microfluidics is a field of science that studies the behavior of fluids at sub-millimeter scale. The dimension of a microfluidic system is in the range of 1 to 1000 micrometer. At this scale, the flow regime in a micro channel is laminar, due to the small Reynolds number, often inferior to unity. [20] Therefore, mass transfer occurs through diffusion providing a higher control of the local concentrations at the two fluid streams boundary, and heat transfer occurs through conduction. Furthermore, the increased surface to volume ratio enhances as well mass and heat transfer which results as well in a better control of operating parameters like temperature and concentration. [17] Consequently, microfluidic crystallizers can yield crystals with a narrow size distribution.

Microfluidic technology also simplifies the integration of analytical and detection equipment in the production system. Crystal formation can thus be followed during all the operation providing online information about the system and the rate processes of crystallization. Moreover, this integration increases process control.

Although these systems are at sub-millimeter scale they can ensure a large production of crystals, due to the ease of numbering up micro channels. For example, recent research showed the ability of parallelize micro channels promoting a feasible scaling out of the microfluidic system. [17]

2.2. Crystal Characterization

Crystal is the name given to the solid product obtained during a crystallization phenomenon. A crystal is characterized by its regular appearance resulting from both short and long-range order of its building blocks and from the symmetry of their arrangement. [11] [21]

The building blocks are the molecules and atoms within the crystal which are held together by short-range order forces known as non-covalent interactions. The smallest building block is called unit cell. All unit cells in a specific crystal are the same size and contain the same number of atoms and molecules arranged in the same way. By simple displacements in three dimensions of the unit cells it is built a crystal lattice (see Figure 2.6). [11] [21]

In order to maximize the attractive interactions between atoms and molecules, and thus minimize the energetic state, only well-defined symmetries in the arrangement of the buildings blocks are possible to build a stable crystal lattice. There are only seven regular well-defined symmetries possible, which are defined as crystal systems (see Figure 2.7). For pharmaceutical

compounds, there are three common types of crystal systems: triclinic, monoclinic and orthorhombic. [11] [21]

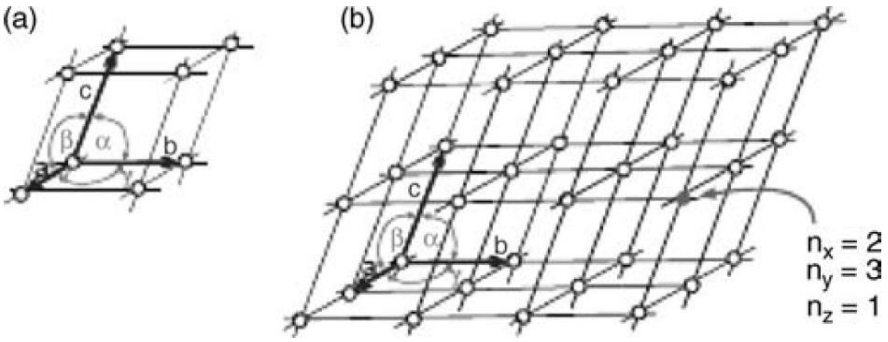

Figure 2.6 Smallest building block of a crystal, (a) unit cell, which is repeated in all three directions via translation forming a (b) crystal lattice. The size of the unit cell is described by the lattice constants a, b, and c, and the angles α, β, and γ. [11]

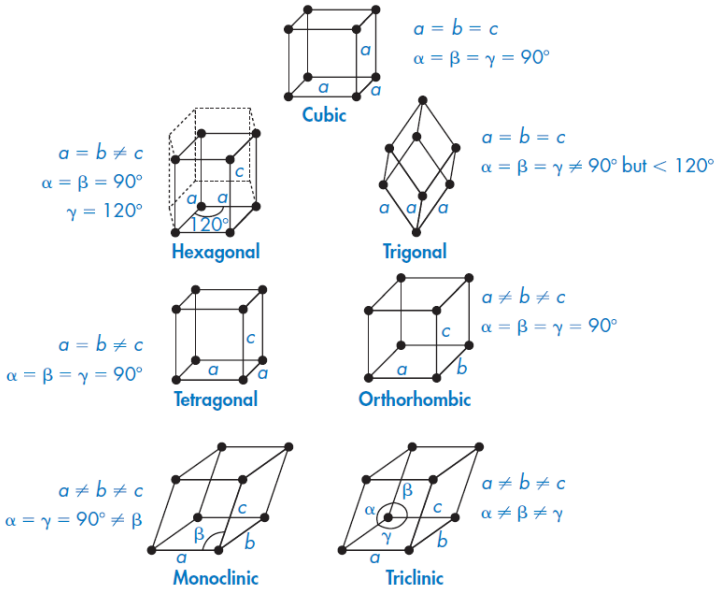

Figure 2.7 The seven possible crystal systems. [21]

The conditions of a crystallization will define the long-range order and the arrangement of the building blocks, and, consequentially, will define the properties and functionality of the solid product. Therefore, it is always necessary to characterize a crystal. If the solid substance will have application in pharmaceutical and food industry, the need of characterization is even higher due to their stringent quality demands. Consequently, a variety of particle characteristics has to be narrowly controlled in order to meet the industrial requirements. Examples of those characteristics are crystal size distribution, crystal habit, polymorph forms, uptake of impurities, and degree of agglomeration.

[11] [13] Some of these properties will be discussed in the following subchapters, as well as the different analysis that can be applied to control them.

2.2.1. Crystal Properties

2.2.1.1. Crystal Habit

The shape of a crystal, also called the habit, corresponds to its external appearance. The crystal habit can be often mistaken by morphology. The crystal habit is related with the relative width and length, and the number of crystal faces. The morphology of a crystal is related with the number of all possible combinations of crystal faces. Nevertheless, the habit of a crystal is dependent on its internal structure. [21]

The shape of a crystal can be classified as acicular (needle-like), platy (plate-like), columnar (like prismatic), pyramidal, tabular, equant, lamellar, among others (see Figure 2.8). [11] [21]

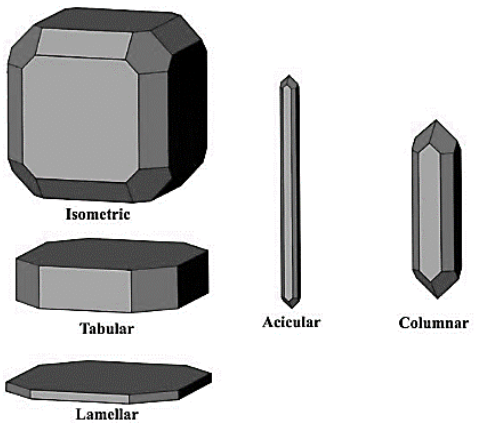

Figure 2.8 Examples of some crystal habits. [21]

The bioavailability of a drug does not present significant differences with distinct habits. On the other hand, differences in the ability to inject a suspension containing a drug in the solid phase are identified for distinct crystal shapes. For example, plate-like crystals are easier to inject through a fine needle than needle-like crystals are. The shape of a crystal also influences the downstream processing characteristics of the solid. For example, acicular crystals exhibit easier tendency to break easily, and thus cause poor filterability. Moreover, tableting can be also compromised due to the change in flow and compaction characteristics promoted by distinct shapes. [11] [13] [21] An example is the powder bridging in the hopper of the tablet machine and the capping problems during tableting caused by the plate-like habit of tolbutamide crystals. [21]

The different shapes of a crystal are a consequence of two factors, a thermodynamic factor and a kinetic factor. The first is related with the structure of the crystal lattice, which is influenced by the bond energies between the building blocks. The second is related with the crystal growth rate, which is affected by the solvent selected for the operation and the presence of impurities in the solution. [13] [21] There are impurities that are desired impurities because they were added to the solvent in order to modify the shape of the crystal. For example, some additives, such as surfactants, can modify the crystal habit by adsorbing onto growing faces during crystal growth. [11] [21]However, the easiest way to modify the shape of the crystal is by changing the solvent in use. The interactions between the solvent and the chemical structure surface of the crystal faces have an important role in shaping a crystal. By modeling, it is possible to know which interactions must be intensified, polar or apolar interactions, and thus, which group of solvents must be used to obtain the desired crystal habit. [11]

2.2.1.2. Crystal Size Distribution, CSD

The crystals of a given solid powder do not possess precisely the same size. In fact, the size of the crystals corresponds not to a single size value but to a range of size values. This range is commonly called as Crystal Size Distribution, CSD, which is one of the most important tools to characterize the size of a solid product. CSD is mainly represented as a number distribution or a mass distribution, which present the total number or mass of crystals between 0 and *L*, respectively. These functions can be displayed as differential or cumulative distributions (see Figure 2.9). [11] [13]

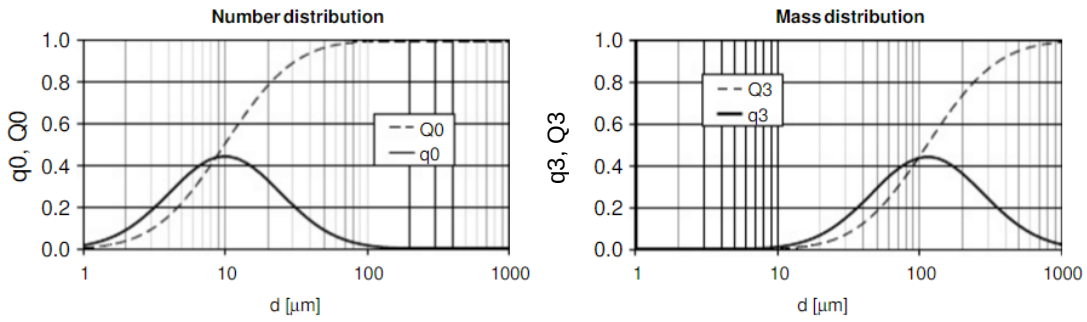

(a) (b)

Figure 2.9 Two different Crystal Size Distribution representations: (a) number distribution and (b) mass distribution. Q_0 and Q_3 are cumulative distribution functions and q_0 and q_3 are differential distributions also known as density functions. [11]

The CSD influences the performance of the product, like dissolution and bioavailability, as well as product quality. For example, when the final product has to be dissolved or digested, small crystals are needed in order to reduce the dissolution time. Therefore, the CSD of the product has to

follow a narrow distribution in the small diameters region. Additionally, CSD also influences the performance of the downstream operation, such as separation of the crystals from the mother liquor, and subsequent drying. In this situation, small crystals are not as suitable as previously. Their large surface area to mass ratio promotes a higher mother liquor adhesion after filtration, resulting in a less pure product after drying. CSD is also essential for storage and handling of the final product. [13] [22]

The Crystal Size Distribution of the solid compound in consideration is mainly manipulated by the degree of supersaturation. [11] [13] [22] Figure 2.10 shows the supersaturation dependence of the crystal size and of the kinetic steps of a crystallization process.

As it can be seen, as the supersaturation increases, besides the initial rise in crystal size, the size of a crystal quickly decreases. For a low degree of supersaturation, the new solid phase in solution will adsorb faster in the surface of the crystals already in solution rather than nucleating. Therefore, the size of the crystals will rise. Further supersaturation of the solution will increase the nucleation rate until this is higher than crystal growth rate. For this situation, the new solid phase will mainly nucleate leading to the production of small crystals. [11] [13]

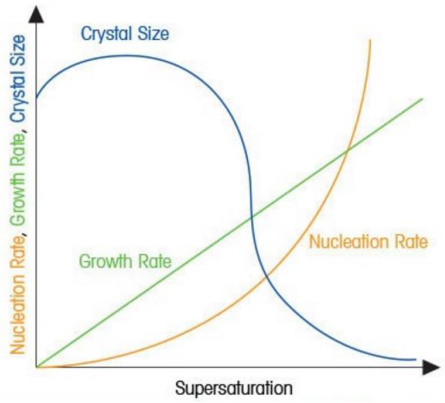

Figure 2.10 Qualitative diagram of the supersaturation dependence of the nucleation rate, the growth rate, and the crystal size, for a secondary nucleation system. [23]

The degree of supersaturation can also influence the crystal shape and the degree of agglomeration. For example, if the supersaturation is slowly induced, large well-formed elongated plates are yield. On the other hand, if supersaturation is quickly induced, fine needles that readily can agglomerate are synthesized. [11] [13]

2.2.1.3. Polymorphism

A singular compound can crystallize as distinct crystal morphologies. This phenomenon is known as polymorphism and occurs when the molecules of a compound are arranged as different

crystal lattices (see Figure 2.7). [11] [13] [21] For simple substances, such as mineral compounds, which have a fixed structure, polymorphism only occurs by different packing arrangements in the crystal lattice. On the other hand, organic compounds have a flexible molecular structure which presents rotational degrees of freedom around a single bond. Therefore, polymorphism can occur, not only by different packing arrangements, but also by different orientation or conformation of the molecules at the lattice sites (see Figure 2.11). [13] [21]

Polymorphs of a given compound are different in morphology resulting in a difference in free energy. Therefore, polymorphs will exhibit distinct physical and chemical properties, as well as distinct mechanical properties. [13] [21] This variation of the properties will strongly influence the processing and the end use of the compound. [13] For example, different structures present different Gibbs free energy of formation which represents the relative stability of the forms. The more stable the polymorph is, the lower is its solubility. Differences in solubility can compromise the bioavailability of the given compound. This fact is one of the reasons why polymorphism is extremely important in the Pharmaceutical industry. [11] [13] [21] Nevertheless, the variation of properties promoted by polymorphism is also relevant for other industries that work with solid compounds. For example, Food industry analyses the possible changes in taste of different forms while Pigment industry studies the color variation promoted by polymorphism. [11] [21]

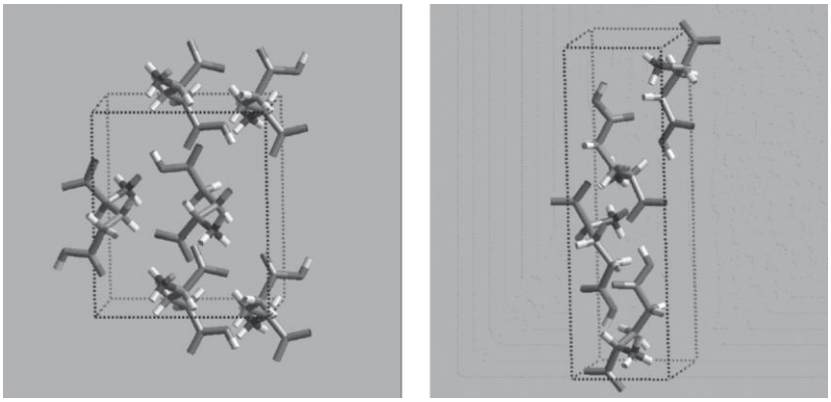

Figure 2.11 Polymorphs of glutamic acid: (a) orthorhombic α-form and (b) orthorhombic β-form. [13]

Polymorphs present different morphologies, and thus will also exhibit different crystal habit. Paracetamol presents two polymorphs which exhibit distinct crystal systems, orthorhombic and monoclinic. The first one has needle-like habit, and the second one exhibits prism and plate habits (see Figure 2.12(a)). The variation of the crystal habit, as mentioned before, can be responsible for compromising the tableting and the injection of the substance. [13] [21]

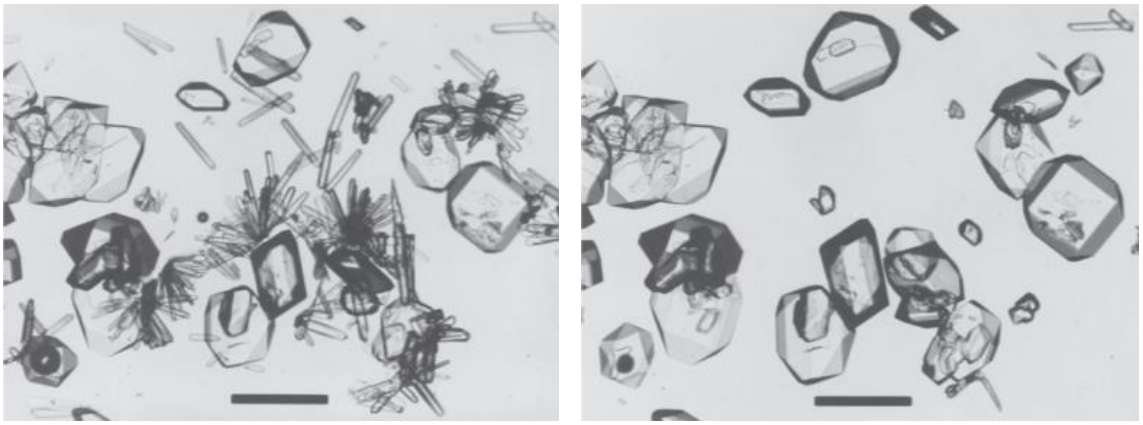

(a) **(b)**

Figure 2.12 Photomicrographs showing the solution-phase polymorphic conversion of orthorhombic paracetamol, needle-like habit, to monoclinic paracetamol, prismatic and platy habits. Micrograph (a) was taken at t = 0 minutes and (b) was taken at t = 30 minutes. The scale bars are equal to 250 μm. [21]

In summary, all solid-state forms of a given compound, as well as their properties, must be acknowledged in order to identify which polymorph offers the desired characteristics. Furthermore, the optimal polymorph must be analyzed to guarantee that it can be produced reproducibly and it does not undergo undesired conversions during its lifetime. [11]

Figure 2.12 also shows a phenomenon that can occur in a polymorphic system. As it can be seen, from picture (a) to (b), orthorhombic paracetamol is transformed into the monoclinic paracetamol. In this particular system, this phenomenon occurred in 30 minutes. However, in other systems, this conversion of the less stable form to the most stable form can occur during processing or storage. To avoid this particular situation, the relative stability of the polymorphs has to be determined. [11] [13] [21]

As mentioned before, the stability of a compound is related with its Gibbs free energy of formation. To study the stability of the different solid-state forms, the Gibbs free energy of formation, G, as well as the thermodynamic state functions of entropy, S, and enthalpy, H, have to be described as a function of temperature, equations 2.6 – 2.8. [11] [13]

$$H\,(T) = H^0 + \int_0^T c_{P,m}(T)\,dT \tag{2.6}$$

$$S\,(T) = S^0 + \int_0^T \frac{c_{P,m}(T)}{T}\,dT \tag{2.7}$$

$$G(T) = H(T) - T \cdot S(T) \tag{2.8}$$

where T is the absolute temperature, H^0 is the enthalpy at 0 Kelvin, $c_{P,m}$ is the molar heat capacity at constant pressure, and S^0 is the entropy at 0 Kelvin.

Furthermore, enthalpy and free energy equations have to be applied to the polymorphs of the given compound as well as to the liquid phase, melt, of the same compound in order to plot them as a function of temperature. Figure 2.13 shows the qualitative energy-temperature diagram of a polymorphic system composed by two polymorphs for two distinct situations. [11]

As it can be seen, in both diagrams the free energy of the liquid phase, G_{liq} , intersects the free energy of both polymorphs, G_I and G_{II}. The intersection points correspond to the melting points of the polymorphs, $T_{m,I}$ and $T_{m,II}$. The identification of the polymorphs is commonly based on their melting points, where the polymorph with the highest melting point is labeled as I, the polymorph with the second highest melting point is labeled as II, and so on. [11] [13]

Figure 2.13(a) represents an enantiotropic system where the free energy curves G_I and G_{II} intersect with each other before any of the polymorphs have achieved its melting point. The intersection point is called transition point because a conversion of the solid form is verified from that temperature. For a temperature below the transition temperature, T_t, polymorph II is the most thermodynamically stable form, $G_{II} < G_I$. Above the transition temperature, G_{II} is higher than G_I. Therefore, polymorph I is then more thermodynamically stable than polymorph II until it achieves its melting point. Figure 2.11(b) represents a monotropic system where an intersection between the free energy curves of the polymorphs is not verified before any of them achieves its melting point. In this system, as $G_I < G_{II}$, the polymorph I is the most stable solid form for all temperature range below its melting point. [11] [13]

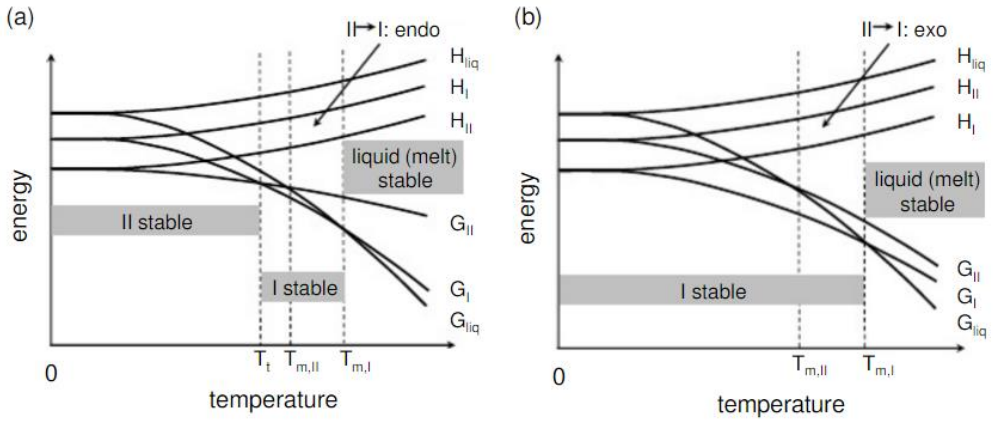

Figure 2.13 Qualitative energy-temperature diagram for an enantiotropic system, (a), and a monotropic system, (b). The temperature regions of the stable forms are also represented. [11]

The identification of a polymorphic system can also be done based on the enthalpy of fusion, according to the Burger-Ramberger fusion rules. If the fusion enthalpy of polymorph I is lower than the fusion enthalpy of polymorph II, $\Delta H_{m,I} > \Delta H_{m,II}$, the system is monotropic (see Figure 2.13(b)). If $\Delta H_{m,I} < \Delta H_{m,II}$, the system is classified as enantiotropic (see Figure2.13(a)). [11] [13]

After discussing the thermodynamics of a polymorphic system, it is important to study the kinetics of the crystallization of polymorphs. As studied previously, see beginning of Chapter 2, to better follow the process of crystallization, the solubility curves of the compounds are needed. [11] [13] Figure 2.14 presents the solubility curves of the two polymorphic systems studied, monotropic and enantiotropic.

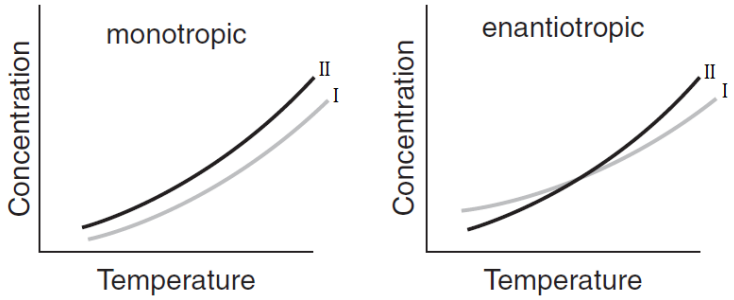

Figure 2.14 Qualitative representation of the solubility curves of a monotropic and enantiotropic system. [13]

As it can be seen, the behavior of the solubility curves is similar to the behavior of the free energy curves for both monotropic and an enantiotropic system. This is a consequence of the relationship between the solubility and the Gibbs free energy, where the solubility of one of the solid-state forms of a given compound is defined as the thermodynamic state where the Gibbs free energy of the solid is equal to the Gibbs free energy of the solid in solution. [11] [13]

For an enantiotropic system, similarly to the free energy curves, the solubility curves also intersect with each other at the transition temperature (see Figure 2.15). This temperature is mainly dependent on the solid crystal lattice structure of the polymorph. The effect of changing the solvent will be only pronounced in the concentration as well as in the width of the metastable region. [11]

As mentioned before, see Chapter 2.1.2, spontaneous nucleation only occurs when the solution is at the limit of the metastable region or beyond it. Therefore, if the metastable regions widths of both polymorphs are overcome during a crystallization operation, the less stable form will crystallize first, according to the Ostwald's rule of stages. This rule implies that the polymorphs will crystallize in sequence from the less stable form to the most stable form. However, this rule was not verified in numerous systems but it is useful for designing polymorphs screens. [11] [13]

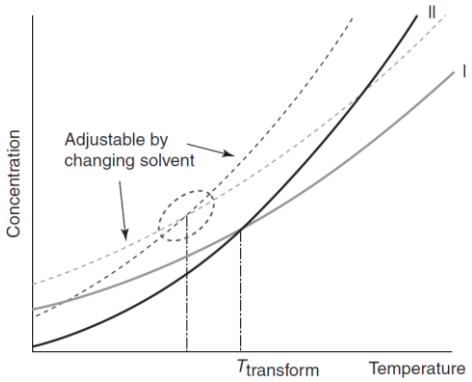

Figure 2.15 Qualitative diagram of the solubility curves of two polymorphs in an enantiotropic system and of the corresponding metastable region limits. $T_{transform}$ corresponds to the transition temperature. [13]

During a crystallization is possible to yield more than one polymorph under similar conditions. This phenomenon is called concomitant polymorphism and can occur when the conditions of the crystallization are near the intersection of the metastability limits. [11]

The reproducibility of the crystallization of a metastable form is quite challenging due to the "disappearing polymorphs". These are polymorphs that can be synthesized at some stage but cannot be reproduced later. In any case, all the possible solid-state forms of a given compound must be identified and characterized in order to avoid serious problems related with unexpected conversion to a new polymorph. [11] [13]

2.2.2. Characterization Methods

2.2.2.1. CSD Characterization [11]

Numerous methods are available to assess CSD. Their selection is dependent on the particle size range of the product in consideration and on the desired information. Examples of methods are Microscopy, Sieving and Laser Light Diffraction.

Microscopy provides information about both shape and size of the crystals. However, it is a very superficial analysis due to the very small amount of crystals that can be analyzed, providing results with large statistical error. Sieving can also be applied to determine CSD. This method continues to be a choice for many measurements because of being simple, inexpensive and of easy interpretation. This technic is based on separating the crystals by sieves of different sizes, where the size range is larger than 20 micrometers. Nevertheless, this method can lead to crystals breakage compromising the crystal size distribution.

The most applied method is laser light diffraction. This method provides a very large size range, excellent statistics and speed, and ease of use. The dynamic range of particle size diameters

goes from 0.2 to 2000 micrometers. Laser light diffraction is suitable for dry powders as well as for suspensions. This technic is based on the principle that particles, when illuminated by coherent light, will scatter light at an angle that is directly related with their size. Therefore, the size distribution is determined from the intensity distribution measured by the proper equipment. Frequently, the CSD representation obtained is a volume distribution of equivalent spherical particles. In other words, the result obtained is a distribution of diameters of spherical particles that interact with the laser light similarly as the nonspherical particles in the sample in consideration. Consequently, when comparing the results of this method with another CSD technic differences may be detected.

2.2.2.2. Polymorphs characterization

A given compound, as mentioned previously, can have distinct crystal structures in solid state, which exhibit distinct properties. This variation of characteristics can compromise the final use of the compound (see Section 2.2.1.3). Therefore, the presence of different structures in the solid powder of the compound in consideration must be verified.

The Powder X-ray Diffraction, PXRD, is the first choice for polymorph characterization. This technic is based on the irradiation of a sample of crystal powder of the given compound with an X-ray beam. The crystal planes within the crystal lattices, when irradiated, they will give rise to a constructive interference at a specific angle. At the end, it will be obtained an average pattern of the angles detected from the crystal structure irradiated, see Figure 2.16. As different polymorphs present different structures, they will exhibit different PXRD patterns. [11]

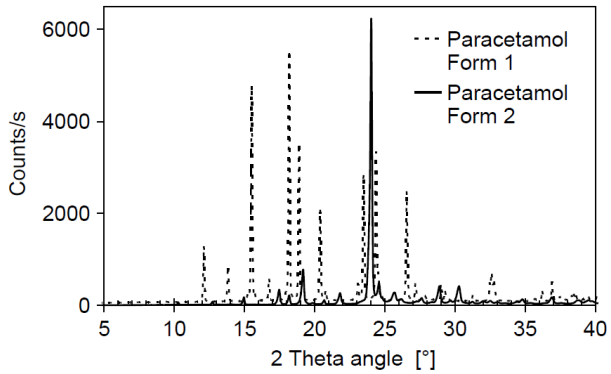

Figure 2.16 PXRD of a sample of paracetamol that exhibits two different solid-state forms. [11]

The particles need to be randomly oriented in order to the crystal planes in the crystal lattice being suitably oriented with respect to the X-ray beam. Otherwise, some of the lines in the PXRD can be highly attenuated or even disappear. To avoid these errors, numerous samples should undergo this method or an additional analysis should be used to be compared with the PXRD information. [11]

Nuclear Magnetic Resonance spectroscopy, NMR, as well as Raman spectroscopy, can be used to provide additional information related to the existence of polymorphs. These technics, unlike PXRD, are sensitive to local order and local properties, i.e. chemical structure. [11]

In Raman spectroscopy, the crystal powder sample is irradiated with a monochromatic laser beam. The molecules of the crystals will interact with the laser beam promoting scattered light. If the scattered light has a different frequency from that of the incident light, it will be used to construct a Raman spectrum, by either measuring the frequency or the intensity of the scattered radiation. The vibrations within the molecules are influenced by the environment of the molecules and the crystal packing. Therefore, as polymorphs have different crystal arrangements, they will have different spectrums, Figure 2.17. [11] [24]

Raman spectroscopy does not require sample preparation and can be easily adapted for online monitoring. Additionally, this spectroscopy analysis readily reaches low frequencies, the characteristic range of lattice vibrations, where the differences between polymorphs is frequently highly pronounced. [11]

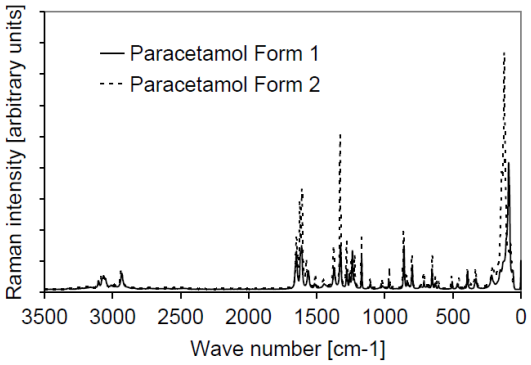

Figure 2.17 Raman spectrum of a paracetamol sample. [11]

NMR spectroscopy is a method that takes advantage of the fact that nuclei of atoms exhibit magnetic properties that can be used to collect chemical information. This method gives chemical-specific structural information and narrow well-resolved bands. However, this method requires a large sample, around 300 mg, and a large time window to obtain the spectrum. Additionally, it is an expensive method. [11] [25]

From a practical standpoint, it is important to determine if a given system is polymorphic, by applying the previous methods or any other, and whether it is monotropic or enantiotropic system. In case of enantiotropic, it is relevant to measure the transition temperature. This information will provide the temperature range at which the desired polymorph is stable, assisting the design of the crystallization and downstream operation to avoid conversion of the solid-form during synthesis and storage. [11] [13]

A thermal method that can be adopted to characterize the polymorph system is a Differential Scanning Calorimetry, DSC. One of the major DSC modes applied is called heat flux DSC. In this mode, the sample and the reference are heated or cooled in different compartments of the same oven and the temperature difference between them it is being measured as a function of temperature. From the temperature difference measured, it is calculated the heat flux difference between the sample and the reference. From this information, a thermogram is obtained where the peaks correspond to a phase transition. If only one peak is observed and it corresponds to a melting phenomenon, the melting temperature is determined accurately by applying a tangent to the melting peak and the correspondent enthalpy of fusion is determined by the area under the peak. [11]

When applied to a polymorphic system, one of three distinct DSC thermograms can be obtained. One of the possible thermograms can only show the melting point and melting temperature of the metastable polymorph. A second possibility is that the thermogram indicates that the metastable polymorph started to melt and was immediately followed by its recrystallization into the high melting temperature form, which started to melt afterwards (see Figure 2.18). The last possibility is that the thermogram describes a solid-solid transition from the metastable to the stable form followed by the melting of the last one. [11]

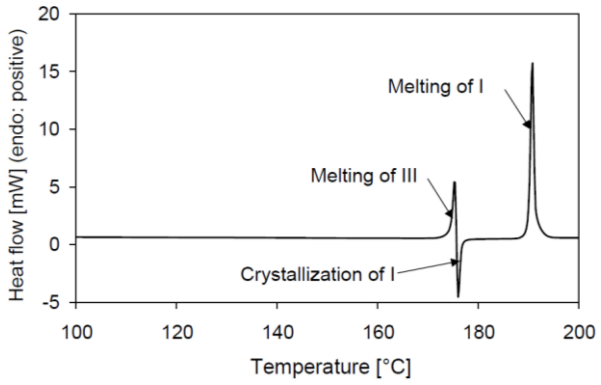

Figure 2.18 DSC thermogram of carbamazepine form III: a solid–solid transition of form III to form I occurs at 170 ºC followed by the melting of form I at 190 ºC. [11]

If from the obtained thermogram it is possible to determine the melting temperatures and the fusion enthalpies of the polymorphs, the system can be characterized into monotropic or enantiotropic by applying the Burger-Ramberger rules. Additionally, an estimate of the transition temperature can be determined by applying specific equations. [11]

Although some compounds can decompose near their melting points, DSC data provides a fast prediction of the relative thermodynamic relationship between the different solid-state forms of a given compound. [11] [13]

Chapter 3

MATERIALS AND METHODS

Imagination is more important than knowledge

Albert Einstein

The aim of this chapter is to describe the experimental methods applied to address the problem under investigation. This chapter is divided in two parts. The first comprehends the methods applied to optimize the unit designed for vitamin D_3 crystallization in continuous micro flow. In this section, the two configurations optimized are explained as well as the two different studies developed for one of the configurations are planned. The second part of this chapter comprehends a brief explanation of the technics adopted to characterize the vitamin D_3 crystals produced under the optimization experiments.

3.1. Continuous micro flow crystallization set-up

A crystallization unit has been designed in this work to intensify the nucleation and the crystal growth separately. Therefore, the set-up is composed by two crystallizers. The purpose of the first crystallizer is to enhance nucleation while the second crystallizer aims to improve and control the crystal growth. The micro flow set-up built for the continuous synthesis of vitamin D_3 crystals is shown in Figure 3.1.

As it can be seen in Figure 3.1, the feed stream of the first crystallizer is a mixture of a solvent with dissolved vitamin D_3 and an anti-solvent. The flow of this homogeneous mixture is manipulated with a valve in order to be fed as droplets. As this way, the surface to volume ratio is increased improving the heat transfer which optimizes the removal of the solvent. The evaporation of the solvent can also be verified in the first layers of the solution when it reaches the bottom of the column.

As mentioned in Section 2.1.2, both evaporation and anti-solvent addition are concentration-driven methods. The evaporation of the solvent, which must have a higher volatility, promotes the increase of vitamin D_3 concentration in the anti-solvent. Furthermore, the vitamin has lower solubility in the anti-solvent. Therefore, the increase in concentration will quickly promote the supersaturation

of the solution. Further evaporation will dramatically increase the supersaturation of the liquid mixture, and thus rise the nucleation rate and nucleus density. The supersaturated solution of anti-solvent and vitamin D_3 is pumped from the first to the second crystallizer, while the solvent evaporated is recycled into the synthesis unit.

The glass column used for the first crystallizer is covered with a heating coil that keeps temperature high enough to promote the evaporation of the solvent while maintaining the anti-solvent in the liquid phase without isomerizing the vitamin.

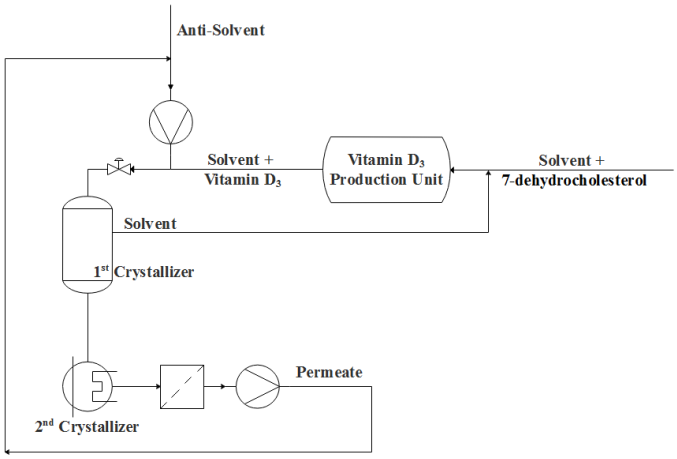

Figure 3.1 Scheme of the unit for vitamin D_3 crystallization in continuous micro flow.

The unit for crystal growth consist of a glass vessel designed to have an integrated cooling jacket that is filled with a cooling liquid. Inside the vessel is the second crystallizer which corresponds to a perfluoroalkoxy, PFA, tube. The vessel is also filled with the cooling liquid to enhance the cooling of the crystallizer.

Flowing from a high temperature to a cooled stage, the solubility of vitamin D_3 in the anti-solvent decreases, increasing the production of solid phase. If the solution is in the metastable region, the solid phase formed in the crystallizer and the remaining clusters produced in the previous vessel will promote the growth of the nucleus into crystals.

After the second crystallizer, a filter is integrated in the system to collect the synthesized crystals. The permeate stream is made of vitamin D_3 dissolved in the anti-solvent and solid phase that did not grow enough to be retained. This stream is recycled to recover vitamin D_3 and is added to the anti-solvent feed of the system.

The explained process was studied in two different set-up configurations. The difference between both is only the equipment used to flow the supersaturated solution through the crystallizer. The following sections will present each configuration and the method associated to study and optimize the crystallization of vitamin D_3.

3.2. Solvent and Anti-solvent selection

The selected solvent was 2-methoxy-2-methylpropane or t-butyl methyl ether. This liquid was selected as a solvent for the vitamin D_3 synthesis step (see Section 1.4). However, as it fulfilled the demands for the crystallization step, high volatility and high solubility of vitamin D_3, it was also chosen for the third step of the project.

Previously to the continuous crystallization study of this thesis, the crystallization of vitamin D_3 was performed in a batch-wise operation with the objective to obtain information regarding the system composed by vitamin D_3 and t-butyl methyl ether. Additionally, the batch crystallization was needed to verify if the continuous process was achievable. Through the crystallization in batch, both anti-solvent and operating temperatures were selected. The later will be approached in the following section.

The selection of the anti-solvent was dependent on two important features. The first one was that the boiling point of the anti-solvent needs to be significantly higher than the solvent in order to allow its successful evaporation without losing any anti-solvent. The second one was that the solubility of vitamin D_3 on the anti-solvent must be lower than the solubility of the vitamin in the solvent. To select the anti-solvent, a variety of liquids was tested in a batch-wise crystallization from which acetonitrile gave the best performance.

Acetonitrile has a boiling point of 82 ºC [26] higher than t-butyl methyl ether, which has 55 ºC [26]. Regarding the solubility of vitamin D_3, Figure 3.2 presents the solubility curve of vitamin D_3 in acetonitrile. As it can be seen, there are two set of curves presented in Figure 3.2. However, this study will use the solubility curve represented by the blue color, because this one was obtained in the batch study mentioned previously.

3.3. Operating conditions

The crystallization of vitamin D_3 is divided in two steps. In the first step, the solvent is removed from the mixture. Therefore, the operating conditions, temperature and pressure, need to be adequate. The pressure selected was 280 mbar and the temperature was 40 ºC. These operating conditions, determined from the batch studies mentioned previously, allow a fast evaporation of the solvent and avoid any vitamin D_3 isomerization. Nevertheless, some anti-solvent can be removed from the mixture during the evaporation.

In the second crystallizer, the temperature needs to be reduced in order to further decrease vitamin solubility in acetonitrile and thus, increment the production of solid phase. The continuous crystallization of the vitamin D_3 was performed for a set of temperatures: 10 ºC, 5 ºC and 0 ºC (see Appendix A). For the first temperature, no crystals were obtained in the filter. This can be a result of

two facts: the mesh of the filter was too small or the temperature was not low enough promoting slow crystal growth and/or very small particles. For the last two temperatures, 5 ºC and 0 ºC, the system clogged. These temperatures allowed the production of a large amount of new solid phase, which, due to a fast crystal growth, resulted in the precipitation of the crystals before the filter. In conclusion, these last temperatures where too low.

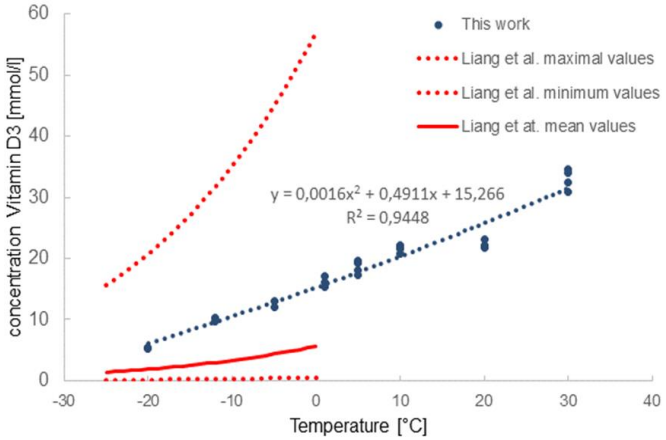

Figure 3.2 Solubility curve of vitamin D_3 in acetonitrile: red curves correspond to the work of Liang et al. and blue curves correspond to the batch study performed for the operation in consideration.

From these results, it was noticed that the crystallizer temperature needed to be a value in between the temperatures tested. Therefore, the second step of the crystallization was tested as well at 7 ºC (see Appendix A). This was the temperature ensuring the best performance and the one selected for further optimization of the system.

3.4. Residence time and volumetric flow rate

The crystallization of the vitamin D_3 was performed in a microscale system. This specific type of system is known by its small residence time in the range of seconds. Therefore, the residence time of the second crystallizer was set for 1 min.

The second crystallizer consists of a PFA tube of 130 mm of length with an internal diameter equal to 1.55 mm. Together with the residence time, the volumetric flow of the system was determined by:

$$\tau = \frac{V}{Q_v} = \frac{\pi \left(\frac{d_i}{2}\right)^2 L_t}{Q_v} \tag{3.1}$$

where τ is the residence time, Q_v is the volumetric flow rate of the mixture, V is the volume of the crystallizer, d_i is the internal diameter of the PFA tube and L_t is the length of the tube.

By applying the equation 3.1 the volumetric flow was rounded to 15 mL h^{-1} (value recognized by the syringe pump) for which the residence time is approximately 59 s.

The volumetric flow rate of the first crystallizer was manipulated manually. Therefore, it was only determined the residence for the second crystallizer.

3.5. Optimization of the vitamin D_3 crystallization process

Optimization is based on the manipulation of the operating conditions and system characteristics to promote higher yield and selectivity. The study presented in this thesis aims to improve the crystallization of vitamin D_3 in continuous flow by manipulating the ratio between anti-solvent and solvent volumes.

3.5.1. Configuration 1 – Single cycle experiments

The experiments started with the preparation of mixtures of pure vitamin D_3, pure solvent and pure anti-solvent (see Table 3.1).

Table 3.1 Quantity of each compound for different mixtures with different anti-solvent/solvent volumes ratios.

Anti-solvent/Solvent volumes ratio	Vitamin D_3 Concentration (mol L^{-1})	Vitamin D_3 Mass (mg)	Solvent Volume (mL)	Anti-solvent Volume (mL)
1.5	0.22	20	0.236	0.355
2				0.473
3				0.709
4				0.945

The concentration of vitamin D_3 was kept constant at 0.22 mol L^{-1}. This concentration value was stablished regarding the specifications of the synthesis step already in development. Additionally, from the first experiments performed, it was noticed that the maximum capacity of vitamin D_3 in the filter was 20 mg. Therefore, the mass of vitamin D_3 added to the mixtures was always the same and equal to 20 mg.

The volume of anti-solvent was determined by the volume of the solvent and the ratio under consideration. The solvent volume was determined from:

$$C_{D_3} = \frac{n_{D_3}}{V_{solvent}} = \frac{m_{D_3}}{V_{solvent} \cdot M_{D_3}} \quad (3.2)$$

where C_{D_3} is vitamin D_3 concentration, in mol L^{-1}, n_{D_3} is the molar quantity of vitamin D_3, m_{D_3} is the mass of vitamin, M_{D_3} is the molar mass of vitamin D_3 (equal to 384.64 g mol^{-1}), and $V_{solvent}$ is the solvent volume, in mL.

Figure 3.3 presents the scheme of the Configuration 1 set-up built to perform the crystallization experiments. Each experiment started by feeding the prepared mixture to the system from the feed reservoir identified in Figure 3.4. From the reservoir, the mixture flows into the first crystallizer with the help of a valve (see Figure 3.5(a)). In this crystallizer, previously heated until 40 ºC, as the mixture flows through the glass column, the t-butyl methyl ether evaporates and it is collected when it condenses. While the solvent is evaporating, the acetonitrile is becoming supersaturated in vitamin D_3. That phenomena can be noticed at naked eye due to a change of color. As the quantity of t-butyl methyl ether decreases in the mixture and the acetonitrile becomes supersaturated, the color changes from transparent to white. Further decrease in solvent content leads to a more intense white color (see Figure 3.5(b)).

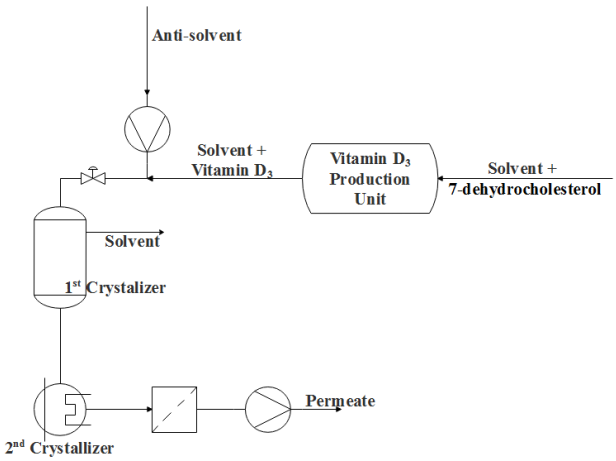

Figure 3.3 Scheme of the Configuration 1 of the set-up built for the crystallization of vitamin D_3.

In this configuration, the acetonitrile, together with vitamin D_3, flows from the first crystallizer towards the second crystallizer with the help of a syringe pump of 6 mL made of stainless steel. This pump is connected to the system at the end of the set-up where it withdraws the permeate stream of the filtration (see Figure 3.4). As the permeate stream has a low content of vitamin D_3 when compared with the supersaturated mixture in the first crystallizer, its color is either slightly white or transparent (see Figure 3.5(b)).

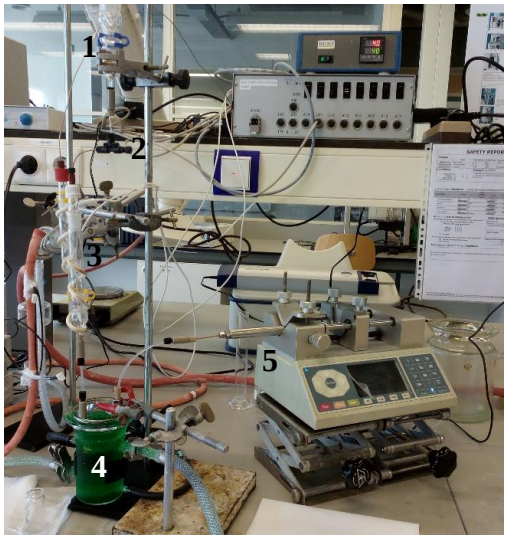

Figure 3.4 Photo of the set-up built for the single cycle experiments: (1) feed reservoir, (2) valve, (3) first crystallizer, (4) second crystallizer, and (5) syringe pump.

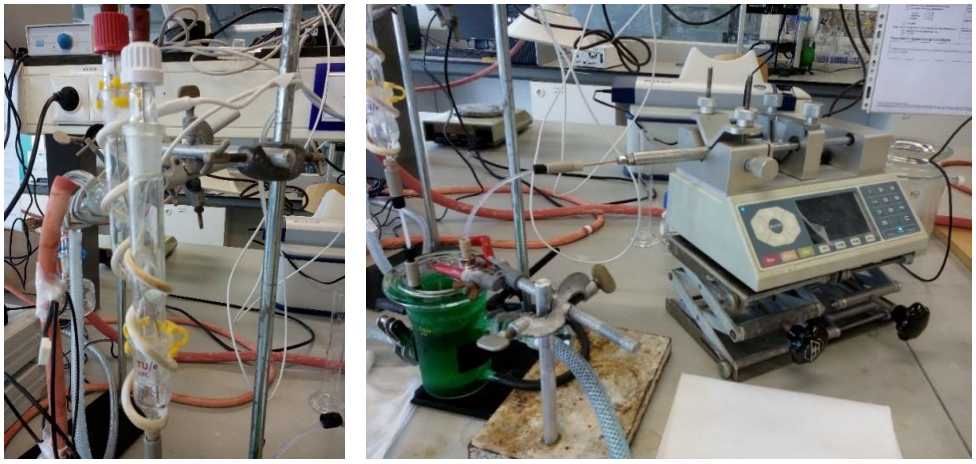

(a) (b)

Figure 3.5 Crystallization set-up for single cycle experiments: (a) first crystallizer, and (b) second crystallizer and the syringe pump.

Each experiment takes approximately 10 minutes. At the end, the filter, previously weighted, is left to dry at room temperature for a while and then is dried with a vacuum pump to make sure that any trace of acetonitrile is removed. Then, the mass of the filter is weighted to measure the quantity of crystals obtained, which are then collected for future analysis (see Section 3.6).

The crystallizer is cleaned with diethyl ether. This compound is a solvent that easily dissolves vitamin D_3, therefore, it is used to collect the precipitated vitamin. The diethyl ether is then removed using a rotavap so the vitamin D_3 can be obtain free of solvent, and then weighted. The latter procedure is also performed with the permeate stream collected by the syringe pump. If there is any residue of mixture in the reservoir where the initial mixture is feed to the system, the reservoir is also

cleaned with diethyl ether and it is then removed in the rotavap. At the end, it is possible to determine the exact quantity of vitamin D_3 that was pumped into the system through global mass balance of vitamin D_3.

Additionally, the absolute yield, equation 3.3, and the filter efficiency of the crystallization process, equation 3.4, can be calculated.

$$\eta_{D_3}(\%) = \frac{m_{filter}}{m_{pumped}} \times 100 \tag{3.3}$$

$$\text{Filter eff.}(\%) = \frac{m_{filter}}{m_{filter} + m_{permeate}} \times 100 \tag{3.4}$$

where η_{D_3} is the absolute yield of the vitamin D_3, m_{filter} is the mass of vitamin D_3 collected in the filter, m_{pumped} is the mass of vitamin D_3 pumped into the system, Filter eff. is the filter efficiency, and $m_{permeate}$ is the mass of vitamin D_3 collected from the permeate stream.

For each anti-solvent/solvent volumes ratio were carried out at least three experiments. The values of filter efficiency and absolute yield for each ratio correspond to an average of the values determined in each experiment.

3.5.2. Configuration 1 – Recycle experiments

At industrial scale the permeate stream is recycled in order to recover the vitamin D_3 and increase process yield. For the purpose of analyzing the recycling effect on the absolute crystals yield and on the filter efficiency, new experiments were run where the permeate stream was reintroduced to the system. The scheme of the of the set-up built for this purpose is presented in Figure 3.6.

These experiments were divided in two parts. The first part, called Cycle 1, was performed exactly as the experiments previously described. At the end, all system was cleaned including the filter. The second part, called Cycle 2, was performed similarly to the first cycle, however, the initial mixture was prepared differently.

The permeate stream is collected at the end of Cycle 1. Then, it is measured the volume of the solution, which is assumed to be the volume of acetonitrile. Considering this volume and the anti-solvent/solvent volumes ratio under study, it is added to the permeate solution the correspondent mixture of t-butyl methyl ether volume with vitamin D_3. The quantity of vitamin D_3 added has to satisfy the concentration defined initially, 0.22 mol L^{-1}, and its calculated through equation 3.2.

The mixture prepared with the permeate of Cycle 1 is then fed to the system starting a new cycle, Cycle 2. When all mixture has been processed, the same procedure explained in the previous section was performed.

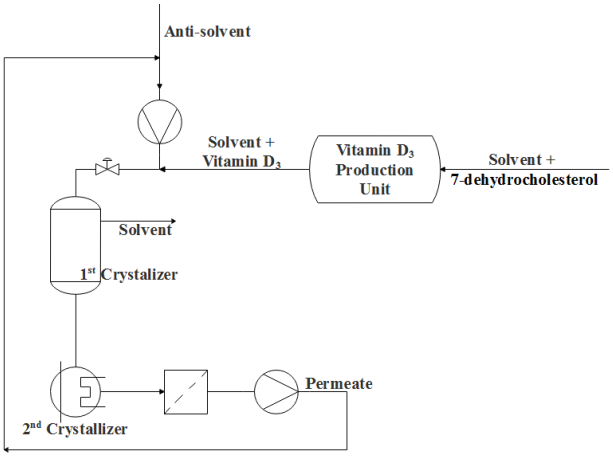

Figure 3.6 Scheme of the Configuration 1 of the set-up built for the crystallization of vitamin D_3 where the permeate stream is recycled.

Applying a mass balance to each cycle, it is possible to determine the mass percentage of the vitamin D_3 in the crystallizer, in the filter and in the permeate for both cycles. Furthermore, the absolute yield, equation 3.3, and the filter efficiency, equation 3.4, are calculated for both cycles.

To be able to compare the results of these experiments with the single cycle results, a global mass balance must be done in order to include both cycles. From the total mass balance, the absolute yield and the filter efficiency are determined:

$$\eta_{D_3}(\%) = \frac{m_{filter,1} + m_{filter,2}}{m_{pumped,t}} \times 100 \quad (3.5)$$

$$Filter\ eff.(\%) = \frac{m_{filter,1} + m_{filter,2}}{m_{filter,1} + m_{filter,2} + m_{permeate,2}} \times 100 \quad (3.6)$$

where, $m_{filter,1}$ and $m_{filter,2}$ are the masses of vitamin D_3 collected in the filter during Cycle 1 and Cycle 2, respectively, $m_{pumped,t}$ is the total mass of vitamin D_3 pumped in both cycles, and $m_{permeate,2}$ is the mass of vitamin D_3 collected in the permeate stream of Cycle 2.

3.5.3. Configuration 2 – Single cycle

During an experiment, the syringe pump cannot guarantee a continuous flow and keep constant the volumetric flow rate. As the filter gets filled with crystals the flow of the acetonitrile-vitamin D_3 mixture starts to reduce compromising the performance of the crystallization. In order to improve the reproducibility of the experiments, a new configuration was used. Instead of using a

syringe pump to circulate the effluent of the first crystallizer, micro peristaltic pumps were used being connected between both crystallizers, as shown in Figure 3.7.

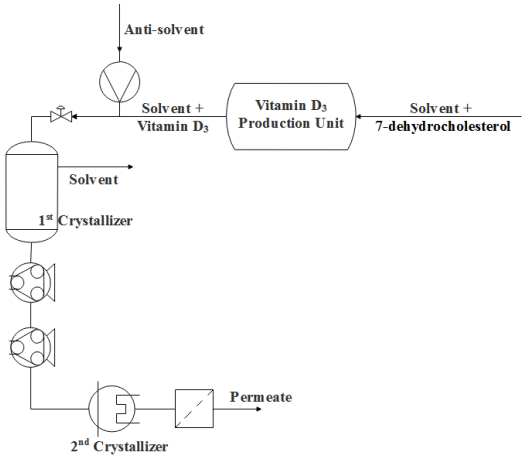

Figure 3.7 Scheme of the Configuration 2 of the set-up built for the crystallization of vitamin D_3.

The experiments performed in this set-up were equal to the ones described for the single cycle experiments.

3.6. Characterization of vitamin D_3 crystals

One of the goals of this project is to produce vitamin D_3 crystals that can be used in dietary supplements. To achieve this goal, the crystals obtained must meet the requirements of the pharmaceutical and food industry concerning those applications. [27] The requirements are related with intrinsic properties, particle shape and size, and mechanical properties (see Section 2.2.1). Therefore, the solid product synthesized needs to be characterized to verify if the crystals satisfy such demands. If the properties analyzed are far from the pharmaceutical requirements, further study of the crystallization process is required in order to obtain the desired crystal's characteristics.

In this thesis, the characterization of the vitamin D_3 crystals consisted in studying the Crystal Size Distribution, the crystals habit and the existence of polymorph forms. The crystal habit will be studied by optical microscope and scanning electron microscope, SEM, pictures, the CSD will be obtained by performing a Laser Light Diffraction, and the existence of polymorphs will be studied through PXRD.

Chapter 4

RESULTS AND DISCUSSION

You cannot teach a man anything; you can only help him discover it in himself.

Galileo

This chapter is divided in two parts. The first part presents the results and discussion of the optimization of vitamin D_3 crystallization. Then the experimental characterization of the obtained vitamin crystals is focused.

4.1. Optimization of the vitamin D_3 crystallization process

As mentioned in Chapter 3, two set-up configurations were developed to address the optimization of the continuous crystallization of vitamin D_3. In the case of Configuration 1, two different studies were performed to demonstrate the yield and filter efficiency improvement achieved by recycling the permeate stream. For Configuration 2, this study was not accomplished due to equipment limitations as explained latter in this chapter.

4.1.1 Configuration 1 – Single cycle experiments

The crystallization was performed for different anti-solvent/solvent volumes ratios. The results shown in Table 4.1 were obtained applying the method described in Section 3.5, namely, the mass percentage of vitamin D_3 obtained in different locations of the system after crystallization, as well as crystals yield and filter efficiency. As it can be seen in Table 4.1, the mass balance for the different ratios never achieves 100% due to losses of vitamin D_3 in the tubing previously to the second crystallizer.

The same points are plotted in Figure 4.1 for better analyzing the behavior of the process characteristics with increasing anti-solvent/solvent volumes ratio. As it can be seen, as the proportion of acetonitrile increases, the crystals yield achieves a maximum value. This behavior, distinct from the trend of the remaining parameters, is related with the decrease of supersaturation degree with the increase of the volume ratio.

Initially, the concentration of vitamin D_3 in the anti-solvent rises as the solvent is removed in the first crystallization stage. For a volumes ratio of 1.5, the acetonitrile will quickly become saturated in vitamin D_3. This fact, together with the low solubility of vitamin D_3 in the acetonitrile, dramatically increases the supersaturation. Consequently, the nucleation rate rises, as well as the nucleus density, driving the solution most probably beyond the metastable limit. In the second crystallizer, the decrease of temperature further reduces vitamin D_3 solubility in acetonitrile promoting the production of more solid phase. As a result, the supersaturation further increases, as well as the nucleation rate. When high nucleation rate is achieved, precipitation can occur. As it can be seen in Figure 4.1, for a volumes ratio of 1.5 most of the vitamin D_3 precipitates in the second crystallizer, 59 %, while only 25 % is obtained in the filter.

Table 4.1 Mass percentage of Vitamin D_3 obtained from a total amount of 20 mg.

	Mass Balance (%)				
Anti-solvent/ /Solvent Ratio	**Permeate**	**Filter**	**2nd Crystallizer Precipitate**	**Absolute yield (%)**	**Filter efficiency (%)**
1.5	3	25	59	25	89
2	22	31	45	31	58
3	34	52	12	52	60
4	47	24	7	24	34

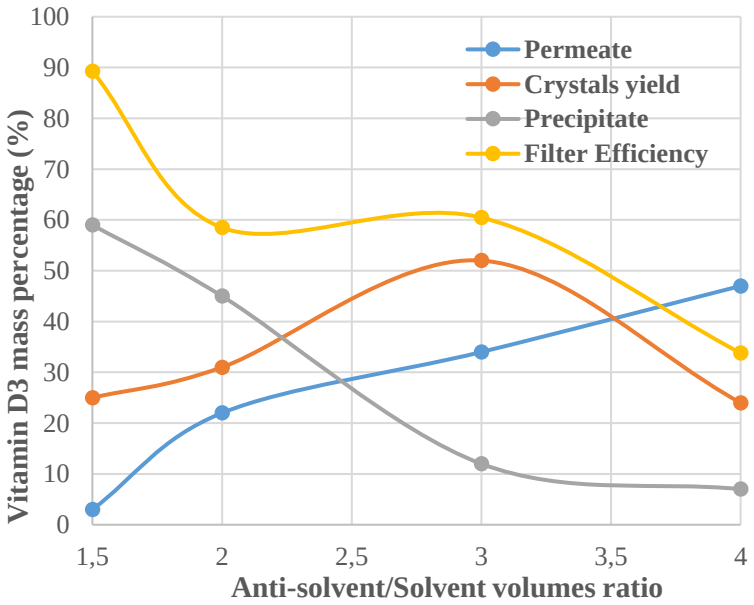

Figure 4.1 Mass percentage of vitamin D_3 obtained from a constant 0.22 mol L^{-1} concentration in t-butyl methyl ether. The experiments were performed in the 2nd crystallizer at a temperature of 7 ºC and 59 s of residence time.

As the anti-solvent/solvent volumes ratio increases, acetonitrile dissolves more vitamin D_3. Therefore, the degree of supersaturation achieved in the first stage of the crystallization decreases, which slows down the nucleation. Consequently, less vitamin D_3 is lost as a precipitate in the crystallizer and more vitamin is collected in the filter as larger crystals. This behavior can be verified in the results obtained (see Figure 4.1). However, for a volumes ratio of 2, the mass percentage of precipitated vitamin D_3 (45 %) is still higher than the one filtered (31 %). As the supersaturation degree decreases, recalling the phase diagram for crystallization from solution (see Chapter 2.1.1), the solution gets closer to the metastable limit. For the situation under consideration, the solution is probably still beyond the metastable region, which explains why precipitation is still important.

For a volumes ratio of 3, a maximum yield of 52 % is reached. This implies that the solution achieves a state where further decrease of the supersaturation degree diminishes the synthesis of crystals while a further increase enables crystals production as well as precipitation. Such state corresponds to the metastable limit. As the crystals yield is higher than the mass of precipitated vitamin, and a further increment of the volumes ratio decreases the mass of filtered vitamin D_3, this may indicate that the solution achieved its metastable limit.

Further increase of the anti-solvent/solvent volumes ratio decreases the amount of filtered vitamin. As mentioned previously, below the metastable limit the nucleation is not spontaneous, and thus the amount of obtained crystals starts to fall. Although the degree of supersaturation is high enough to produce new solid phase, not all solid clusters possess enough energy to generate nucleuses and grow further. Additionally, a higher ratio implies also higher volume of anti-solvent, which can dissolve more vitamin D_3 as explained below. As it can be seen, for a volumes ratio of 4 most of the vitamin is obtained in the permeate stream and the amount of crystals produced drops. It is known that vitamin D_3 has low solubility in acetonitrile but there is still a mass of vitamin that dissolves in it. For instance, at 7 ºC vitamin D_3 solubility is 7.2 mg mL^{-1} (see Appendix B). Therefore, one may estimate the amount of vitamin that is expected to be lost dissolved in the permeate stream. If that amount is excluded from the mass balance (see Appendix B), the absolute yield of the process jumps from 52 % to 70 % as shown in Figure 4.2.

In 2012, Zhang et. al developed a two-stage mixed-suspension mixed-product removal (MSMPR) continuous anti-solvent and cooling crystallization for a pharmaceutical intermediate. [28] Two different configurations were studied: the first one, Configuration A, starts with cooling crystallization and follows with simultaneous cooling crystallization and anti-solvent addition; the second one, Configuration B, starts with both cooling and anti-solvent crystallization, and in a second stage further cooling is performed. This crystallization is similar to the one presented in this thesis concerning the crystallization from solution methods applied to induce supersaturation. Nonetheless,

they are applied differently, and the continuous crystallization was not performed at microscale level, which influences the results. Nevertheless, Zang et. al crystallization experiments yield 92 % of the compound with purity greater than 98 %. [28]

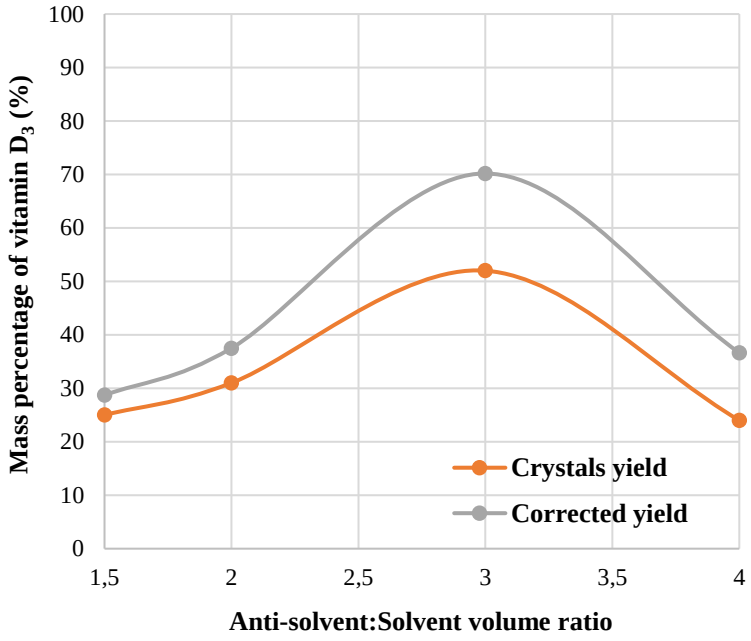

Figure 4.2 Yield of crystallization taking or not into account the solubility of vitamin D_3 in acetonitrile (7.3 mg mL^{-1} at 7 ºC).

When comparing our results (yield of 70 %) with those of Zang et. Al (92 %), there is a significant difference and space for improvement. A possibility for increasing the absolute yield is to recycle the permeate stream in order to recover the vitamin D_3 in solution that can still be crystallized.

Concerning the filter efficiency, Figure 4.1 shows that the efficiency decreases by increasing the anti-solvent/solvent volumes ratio. The filter efficiency, defined by equation 3.4, is the quotient between the mass of vitamin D_3 crystals collected in the filter and the total mass of vitamin feed to the filter unit. When the volume ratio varies from 1.5 to 2, there is a significant increase in the mass quantity of vitamin D_3 in the permeate (see Figure 4.1) which promotes a decrease in the filter efficiency. For a volumes ratio of 4, the permeate has a higher amount of vitamin than the filter, and thus the efficiency decreases significantly. The decrease of filter efficiency is a result of the increase in acetonitrile volume, which increases the amount of vitamin dissolved in the solution. Nevertheless, developed crystals can also be present in the permeate stream which could be too small to be retained in the filter. Therefore, filter efficiency could be improved by reducing the mesh of the filter to

increase vitamin D_3 crystals collection. Nonetheless, it must be taken into account the possible increase in back pressure.

In summary, the best crystallization performance was obtained for an anti-solvent/solvent volume ratio of 3 that yields 52 % of crystals (see Figure 4.2) with only 12 % of loses as precipitated.

4.1.2 Configuration 1 – Recycle experiments

As mentioned above, the Recycle experiments were performed to analyze the improvement in crystals yield and filter efficiency when compared with single cycle experiments.

Applying the procedure described in Section 3.5.2, the mass percentage of vitamin D_3 was determined and compiled in Table 4.2.

Table 4.2 Mass percentage of Vitamin D_3 obtained from a total amount of 75 mg (0.22 mol L^{-1} in t-butyl methyl ether, solvent).

			Mass of Vitamin D_3 (%)		
Anti-solvent/ /Solvent Ratio	**Essay**		**2nd Crystallizer Precipitate**	**Filter**	**Permeate**
3	Recycle experiment 1	Cycle 1	9	13	78
		Cycle 2	28	6	46
	Recycle experiment 2	Cycle 1	14	27	59
		Cycle 2	24	15	56

The results for the Cycle 1 were expected to be similar to those obtained during the Single cycle experiments for the same volumes ratio (ratio of 3). Recalling the results of Single cycle experiments, the mass percentage of vitamin D_3 were 12 % in the crystallizer, 52 % in the filter and 34 % in the permeate. As it can be seen, during the Recycle experiments most of the vitamin D_3 was obtained in the permeate stream instead of in the filter as expected. This difference indicates that the residence time in the first crystallizer was not enough. The nucleation enhancement in the first crystallizer is denominated as primary nucleation and its rate is known to be slow for low supersaturation. Therefore, a short residence time does not allow the generation of a high amount of nucleus. When the solution enters in the second crystallizer, due to the small amount of nucleus, most of the vitamin D_3 will remain in solution and the amount of crystals obtained will be really small.

Recycling the permeate stream increases the quantity of vitamin D_3 at the inlet of the first crystallizer. The high concentration of vitamin D_3 promotes a faster supersaturation of the solution vitamin D_3-acetonitrile as the solvent is removed. A high supersaturation results in high nucleation rate, rising the nucleus density in solution. As the solution flows through the second crystallizer the

temperature reduction will promote the separation of vitamin D_3 as crystals. The crystals that do not precipitate will be collected in the filter. Therefore, from the Cycle 2 it is expected that most of the vitamin D_3 is obtained as a precipitate in the second crystallizer and as crystals in the filter. As it can be seen, the quantity of vitamin D_3 in the second crystallizer increases from Cycle 1 to Cycle 2 and the quantity of the vitamin in the permeate decreases. However, vitamin D_3 is mostly found in the permeate stream and it was expected to be mostly found precipitated in the system. A possible cause for this behavior is the same as for Cycle 1, i.e. the residence time in the first crystallizer was not long enough.

The crystals yield and the filter efficiency of each cycle for the Recycle experiments are presented in Table 4.3. As analyzed above, the amount of vitamin D_3 in the filter was reduced and the vitamin D_3 present in the permeate stream was higher than expected in both cycles. Consequently, the filter efficiency from each cycle is small as well as the absolute crystals yield.

Table 4.3 Absolute crystallization yield and filter efficiency of each cycle for the Recycle experiments.

			Mass of Vitamin D_3 (%)	
Anti-solvent/ /Solvent Ratio	**Essay**		**Absolute yield (%)**	**Filter efficiency (%)**
3	Recycle experiment 1	Cycle 1	13	14
		Cycle 2	6	12
	Recycle experiment 2	Cycle 1	27	31
		Cycle 2	15	21

After performing a mass balance for each Recycle experiment, it was determined the absolute yield and filter efficiency of the complete experiment. Comparing these values with those for Single cycle experiments – see Table 4.4 – on may conclude that a unique cycle is better than recycling the permeate stream.

Table 4.4 Comparison of absolute yield and filter efficiency between Single cycle experiments and Recycle experiments.

Anti-solvent/Solvent Ratio	**Experiment**	**Absolute yield (%)**	**Filter efficiency (%)**
3	Single cycle	52	60
	Recycle 1	14	26
	Recycle 2	28	41

Nonetheless, *a priori*, recycling the permeate stream should increase both yield and efficiency, being expected to obtain better results than with a single cycle. The amount of experiments performed was not enough to take a strong conclusion about recycling permeate stream. More experiments must be carried out for a better perception of the behavior of both crystal yield and filter efficiency with recycling. Nevertheless, this experiments exhibit the poor reproducibility of this crystallization process. A possibility of improvement can be improving the pumping system of the configuration under study.

4.1.3 Configuration 2 – Single cycle experiments

Initially, one micro peristaltic pump was not enough to flow the solution through the filter. Two pumps were also not enough to overcome the backpressure created by the filter. There were only two pump's controllers available. Therefore, using more pumps was not an option. The only options were either connect two filters in parallel or using a filter with higher surface area. Due to money and time limitations the second option was adopted. The increase of surface area helped decrease the backpressure. Consequently, the pumps had enough energy to flow the mixture through the filter.

After optimizing the set-up, the settings of the peristaltic pump, amplitude and frequency, needed to be tested to verify which pair of settings corresponds to the desired volumetric flow rate. However, for any pair of settings the flow rate was always equal to 1 mL min^{-1}. After discussing this situation with the supplier, it was understood that, in order to be able to use the pumps properly, the system needed to be filled first with the solution. To fill the system, a syringe pump should be added to this configuration. At the end, the configuration would start as the previous configurations to further evolve into a new one, which would not be practical. Therefore, at the end, it was decided not to study this configuration.

4.2. Characterization of vitamin D_3 crystals

As has been mentioned above, the crystal habit, crystal size distribution, and polymorphism are the main crystal properties under analysis in this project. The crystals of vitamin D_3 produced during the Single cycle experiments for a volume ratio of 3 were collected in order to analyze their quality. Only these crystals have been analyzed because they correspond to the solid produced under the best crystallization performance.

4.2.1. Crystal Habit

In order to identify the crystals habit of the produced vitamin D_3, both optical microscopy and scanning electron microscopy pictures were taken – see Figures 4.3 and 4.4, respectively.

Figure 4.3 shows crystals exhibiting a prismatic habit. However, in Figure 4.4(a) some crystals, among the prismatic ones, possess a very small width, similar to needle-like crystals. Hence it is not clear the real habit of vitamin D_3 crystals.

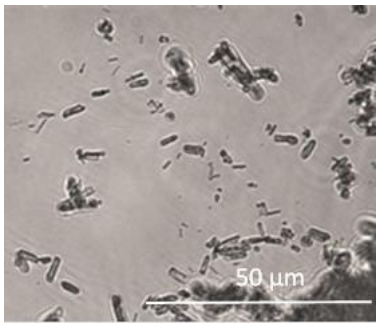

Figure 4.3 Optical microscopy picture of vitamin D_3 crystals obtained from experiments with anti-solvent/solvent volumes ratio of 3.

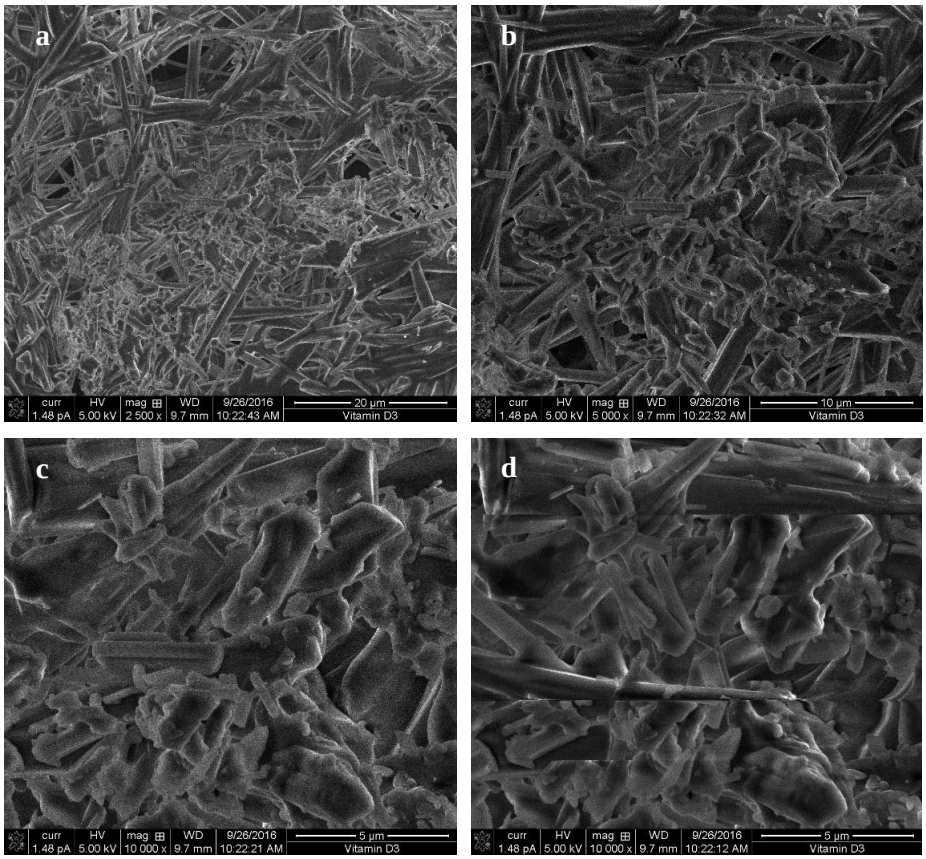

Figure 4.4 SEM pictures of a sample of vitamin D_3 crystals obtained from experiments using anti-solvent/solvent volumes ratio of 3. (a) 20 µm scale, (b) 10 µm scale, and (c) and (d) 5µm scale.

However, as the scale of the SEM pictures of Figure 4.4 diminishes, it becomes more clear that the crystals shape is prismatic. Both needle-like and prismatic crystals grow essentially in length, but the prismatic ones are thicker than the needle-like crystals, and the edges are round rather than needle-like. Such different habits can be sometimes easily confused.

It was mentioned in Section 2.4 the disadvantages of some crystals habit. For example, crystals with needle-like habit are unsuitable for downstream operations, and platy-like crystals will impair tableting process. No disadvantages were found concerning prismatic habit. However, needle-like and prismatic habits are close and may present a similar poor hydrodynamic behavior. Nevertheless, in principle, the prismatic crystals may be suitable for the various steps after crystallization operation until their final application.

Besides the shape of the crystals, Figures 4.3 and 4.4 also reveal a high degree of agglomeration between the crystals, which occurs when particles collide and the attractive forces between them are superior than the repulsive forces. Agglomeration is not a desire crystal characteristic due to the mother liquor that is contained within the primary crystals of the agglomerate. That mother liquor is difficult to separate during drying, and promotes caking of the product during storage. Additionally, agglomerates break more easily than solid crystals, and release solvent during their breakage. [11]

During crystallization, the occurrence of agglomeration depends on the degree of supersaturation of the solution. The higher is the supersaturation degree, the higher is the probability for agglomeration and the stronger is the binding between agglomerated particles. In order to reduce the agglomeration observed in the previous pictures, the crystallization experiments must run under low degree of supersaturation. Considering the results obtained for the optimization of the crystallization process, when the anti-solvent/solvent volumes ratio increases, the supersaturation level decreases. Nevertheless, the yield suffers a large reduction as well. For example, from a volume ratio of 3 to 4, the absolute yield decreases from 52 % to 24 %.

The degree of supersaturation can be also attenuated reducing the temperature difference between the two crystallizers. For instance, if the second crystallizer operates at room temperature, the decrease of vitamin D_3 solubility in acetonitrile is lower, when compared with the solubility at 7 ^{o}C, which results in lower amounts of new solid phase. Consequently, the degree of supersaturation decreases. Nonetheless, the yield will also decrease since at higher temperatures the solubility of vitamin is also higher, promoting more loses of vitamin dissolved in the anti-solvent.

Reducing the residence time (i.e. incrementing the volumetric flow rate) could also hinder crystals agglomeration because it would provide less time for the particles to grow, thus reducing the probability of agglomeration in the second crystallizer. However, high volumetric flow rates can promote crystals precipitation, clogging the system.

In summary, experiments for 3 and 4 volumes ratios may be performed under shorter residence times and/or higher operating temperature in order to disclose the effect on agglomeration. Additionally, the characterization of crystals produced during Recycle experiments should also be accomplished to verify if this mode of operation has any effect on both crystal habit and agglomeration.

4.2.2. Crystal Size Distribution

Figure 4.5 reveals crystals with a substantial size distribution. To better analyze the size of the crystals, a laser light diffraction method was applied to a sample of vitamin D_3 in order to obtain the crystal size distribution, CSD. Figure 4.5 presents the obtained CSD, displayed as a density function, where the mean particle size value is equal to 15.03 ± 0.31 μm. As it can be seen, the size distribution is substantially wide. The extent of particle sizes goes from approximately 0.25 μm to almost 500 μm which is not desired.

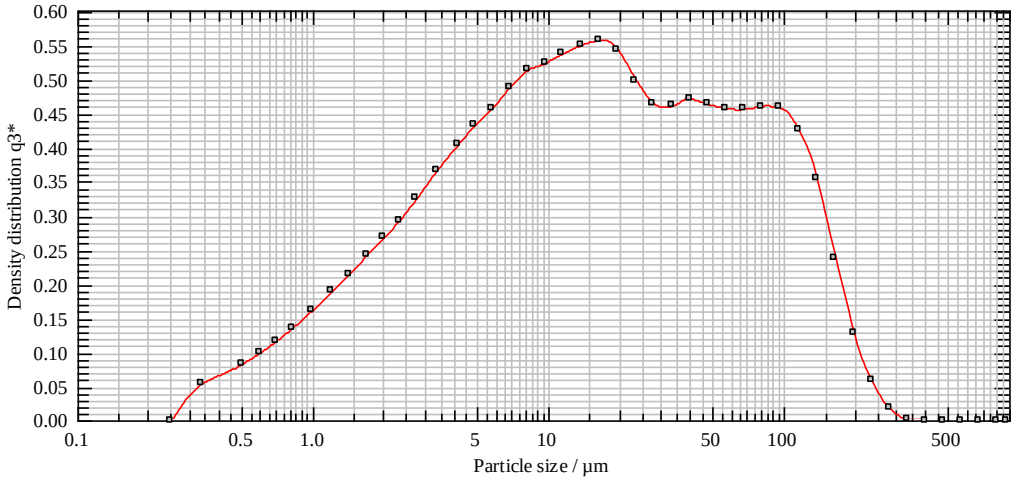

Figure 4.5 Density function obtained from laser light diffraction of the vitamin D_3 crystals produced during a 3 volumes ratio experiment.

The desired result would be a narrow distribution of small particle sizes. The smaller the size, the better the performance of the crystals from a bioavailability point of view. Additionally, if the crystals are too large, like 500 μm, the crystallizer will be clogged due to its small internal diameter, 1.55 mm.

To produce small crystals, both nucleation and crystal growth rates must be high, which means the degree of supersaturation should be high. As mentioned before in this chapter, at a volumes ratio of 3, the supersaturation is high as desired for small crystals production, but the obtained CSD indicates the presence of large crystals in the final product. This problem may be solved increasing

the volumetric flow rate of the feed (i.e. reducing the residence time), and/or increasing the temperature in the second crystallizer to increase solubility. Attention must be paid to the increase of the temperature of the second crystallizer since, as highlighted before, the vitamin solubility in the anti-solvent increases, and the global yield is unfortunately penalized.

In summary, experiments for a volume ratio of 3 can be performed under shorter residence time and/or higher operating temperature in order to obtain narrower crystal size distribution and smaller crystals.

4.2.3. Polymorphism

Vitamin D_3 was known to exhibit only one solid form (form A), whose crystal structure is composed by two different conformers, α and β. In 2016 Wang and coworkers were investigating if the α conformer was responsible for the characteristic chemical instability of vitamin D_3, and found that this vitamin possesses a second solid form (form B). Figure 4.6 presents the PXRD patterns of both forms A and B. [29]

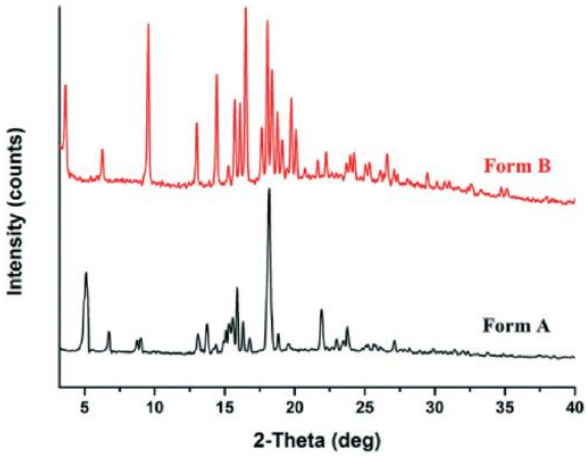

Figure 4.6 PXRD patterns of the two solid forms of vitamin D_3 characterized by Wang and his coworkers. [29]

After the 3 volumes ratio experiments were finished, a sample of these crystals was collected for PXRD analysis. Additionally, a sample of commercial vitamin D_3 purchased from VWR, the same one used for the initial mixtures, was also inspected for comparison, as shown in Figure 4.7.

When the patterns shown in Figures 4.7 and 4.6 are compared, it can be verified that the crystals synthesized in this work correspond to form B while the commercial sample corresponds to form A.

Besides identifying the polymorph form of the crystals, it is also necessary to study the relative thermodynamic stability of the different solids to identify the most stable form. To compare

the stability of both forms, a DSC essay was carried by Wang and coworkers, being possible to identify monotropic or enantiotropic polymorphs. The form A has a melting point of 84 ºC while form B equals 63 ºC. Considering these melting points and the fusion enthalpies also determined by the DSC analysis, the energy-temperature diagram Figure 4.8 was built. [29]

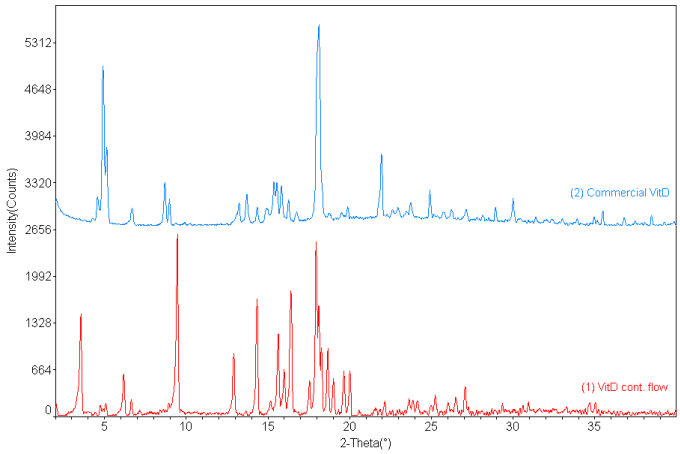

Figure 4.7 Powder X-ray diffraction pattern of (1) vitamin D_3 crystals synthesized during experiments for a volumes ratio of 3 and (2) a commercial sample of vitamin D_3 purchased from VWR.

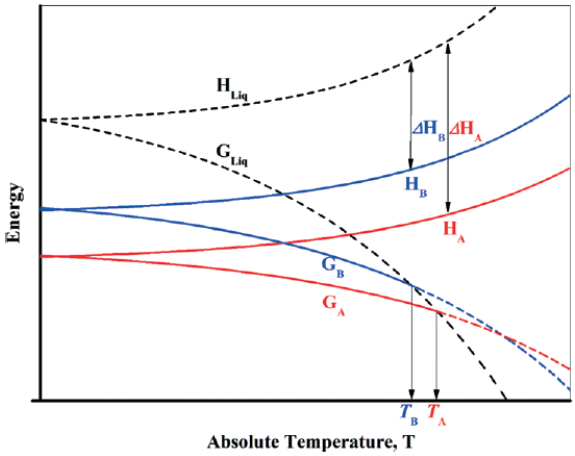

Figure 4.8 Energy-temperature diagram obtained for the two solid forms of Vitamin D_3, form A and form B. [29]

As can be seen from Figure 4.8, the relative thermodynamic behavior of vitamin D_3 solid-state forms correspond to a monotropic system, where form B is the less stable one. Therefore, its synthesis must be avoided in order to prevent conversion of form B into form A.

Wang et al. obtained the solid-state form B from a supersaturated acetonitrile solution at 5 ºC, where prism-like highly crystalline form B was obtained together with form A. Further study has revealed that pure form B can be synthesized using alcohols as solvent and performing the

crystallization at -20 ºC. Wang et al. concluded that polar solvents and lower temperatures were advantageous for synthesizing form B. [29] Therefore, two alternatives are available to prevent the form B synthesis by the crystallization process of this study. Wang et al. obtained form B using acetonitrile, the anti-solvent selected for the crystallization in study. Therefore, an alternative can be changing the anti-solvent for another organic liquid where vitamin D_3 has lower solubility. A second alternative is increasing the temperature of the second crystallizer. Wang et al. obtained form B at 5 ºC. The crystallization in study was performed at 7 ºC, a temperature still close to the operation developed by Wang et al., hence the crystallization could be, for example, performed at room temperature. Nevertheless, it is important to remember that at 10 ºC the crystals were not retained in the filter (see Section 3.3). However, it was not concluded if crystals were produced or not, it only indicates that crystals were not large enough to be retained in the filter. Therefore, if experiments were performed at room temperature (ca. 19 ºC), a smaller filter mesh, 2 μm or 0.5 μm, must be used to guarantee vitamin D_3 crystals collection.

In summary, the crystals produced by the crystallization process of this thesis, unlike the vitamin D3 obtained from VWR, correspond to the less stable solid-state form of vitamin D_3, form B. This form can be converted into the most stable one, form A, by manipulating the temperature of the second crystallizer or by changing the anti-solvent.

Chapter 5

CONCLUSION AND FURTHER RESEARCH

If you believe in yourself first, you're unstoppable

Mendell Grinter

This chapter contains the main conclusions of the study accomplished to optimize a continuous micro flow unit for crystallization of vitamin D_3. Moreover, some different approaches are presented with the objective to improve vitamin D_3 crystallization at a sub-millimeter scale.

5.1. Conclusions

In this project a two-stage crystallization unit was proposed and optimized in order to produce crystals of vitamin D_3 under continuous operation. This is a novel crystallization process and has been implemented under microfluid conditions to take advantage of the better control and manipulation of the kinetics of crystallization, as well as enhance mass and heat transfer due to the inherent high surface to volume ratio. In the first stage of the unit, a simultaneous solvent evaporation and anti-solvent addition are performed to enhance nucleation, while in the second stage the crystal growth is enhanced by cooling.

Two configurations of the unit were considered to verify if reproducibility of the crystallization process could be improved. In Configuration 1 the supersaturated solution was pumped by a syringe pump, while in Configuration 2 the solution was pumped using a micro-peristaltic pump. The later presented some equipment limitations, which solution was not practical for the design in study (see Section 4.1.3). Therefore, only Configuration 1 was studied.

The optimization of the crystallization of vitamin D_3 was accomplished by studying the influence of the ratio between the anti-solvent (acetonitrile) and the solvent (t-butyl methyl ether) volumes on the separation. From the four ratios studied, the volumes ratio of 3 achieved the best

absolute yield (52 %), for which the filter efficiency was 60 %. As there was 48 % for improvement, and since 34 % of vitamin was lost in the permeate stream, additional experiments were carried out recycling this stream to increase global yield and filter efficiency. However, the results were not conclusive, which implies that more essays are required for a decisive investigation.

The vitamin D_3 crystals produced under the best operating conditions were characterized in order to verify if they meet the pharmaceutical industry requirements. Accordingly, crystal habit, crystal size distribution, and the existence of polymorphs were subsequently focused. The vitamin crystals possess a prismatic habit, as well as a high degree of agglomeration. The crystal size distribution measured by laser light diffraction was significantly wide, from ca. 0.25 to 500 μm. Concerning polymorphism, vitamin D_3 had two solid-state forms, named A and B. Form B is the less stable, but it was the form obtained by the crystallization process under analysis. In the whole, these results/characteristics demonstrate that the produced vitamin D_3 crystals are not yet suitable for pharmaceutical application. Nevertheless, there is still room for improvements, mainly if one takes into account this was an exploratory research. On may cite, for example, the reduction of the residence time of the supersaturated solution in the crystallizers, or the increment of the temperature of the second crystallization stage. One should also consider the possibility to substitute the anti-solvent (acetonitrile) for another organic liquid.

5.2. Suggestions of future work

Since the crystallization of vitamin D_3 was already performed at micro scale, it could be assisted by segmented flow. Accordingly, an immiscible fluid is inserted in the main stream with the objective to segment that stream.

In 2015, a variety of studies were published presenting improvements based on crystallization by segmented flow. Due to the small diameter of the micro scale crystallizers, the probability of sedimentation and further clogging of the flow is quite high. Applying segmented flow, this particular situation is avoided because the transport of all crystals is ensured eliminating the production of precipitates during the process. [30] Additionally, uniform sized crystals were observed within each slug. This was as a consequence of the recirculation, where the slurry in each slug is well mixed even in the absence of any static mixer. [30] [31] [32].

As has been mentioned in the conclusions section, several approaches can be analyzed in detail, namely, the influence of feed flow rate (i.e., mean residence time), temperature of cooling crystallization, and nature of anti-solvent upon the final yield, filter efficiency and vitamin D_3 crystal features. Additionally, further research must be done to significantly improve the reproducibility of this process.

REFERENCES

[1] D. L. Nelson and M. M. Cox, Lehninger Principles Of Biochemistry, New York: W. H. Freeman and Company, pp. 360, 2008.

[2] I. Bendik, A. Friedel, F. F. Roos, P. Weber and M. Eggersdorfer, "Vitamin D: a critical and essential micronutrient for human health", *Frontiers in physiology*, vol. 5, pp. 83-96, 2014.

[3] P. Lips, N. M. van Schoor and N. Bravenboer, "Vitamin D-related disorders", in *Primer On The Metabolic Bone Diseases And Disorders Of Mineral Metabolism*, Clifford J. Rosen, pp. 613-623, 2013.

[4] W. B. Grant, H. S. Cross, C. F. Garland, E. D. Gorham, J. Moan, M. Peterlik, A. C. Porojnicu, J. Reichrak and A. Zittermann, "Estimated benefit of increased vitamin D status in reducing the economic burden of disease in western Europe", *Progress in Biophysics and Molecular Biology*, vol. 99, pp. 104-113, 2009.

[5] J. Hilger, A. Friedel, R. Herr, T. Rausch, F. Roos, D. A. Wahl, D. D. Pierroz, P. Weber and K. Hoffmann, "A systematic review of vitamin D status in populations worldwide", *British Journal of Nutrition*, vol. 111, pp. 23-45, 2014.

[6] "Vitamin D Council", [Online]. Available: https://www.vitamindcouncil.org/about-vitamin-d/how-do-i-get-the-vitamin-d-my-body-needs/#. [Accessed December 2016].

[7] M. Juonala, A. Voipio, K. Pahkala, J. S. A. Viikari, V. Mikkilä, M. Kähönen, N. Hutri-Kähönen, A. Jula, B. David, M. A. Sabin, J. Marniemi, B.-M. Loo, T. Laitinen, E. Jokinen, L. Taittonen, C. G. Magnusse and O. T. Raitakari, "Childhood 25-OH vitamin D levels and carotid intima-media thickness in adulthood: the cardiovascular risk in young finns study", *The Journal of Clinical Endocrinology & Metabolism*, vol. 100, pp. 1469–1476, 2015.

[8] A. W. Norman, Vitamin D: The Calcium Homeostatic Steroid Hormone, Elsevier, pp. 60-62, 2012.

[9] F. J. Francis, Wiley Encyclopedia Of Food Science And Technology, 2nd ed., vol. 4, John Wiley & Sons, Inc., 1999.

[10] MarketsandMarkets, "Vitamin D market by analog (vitamin D2 & vitamin D3), application (functional food & beverage, pharmaceuticals, feed & pet food, and personal care), end–user (children, adult, and pregnant women) & by region - global trends & forecast to 2020", 2015.

[11] W. Beckmann, Crystallization: Basic Concepts And Industrial Applications, Wiley - VCH, 2013.

[12] J. Chen, B. Sarma, J. M. B. Evans and A. S. Myerson, "Pharmaceutical crystallization", *Crystal Growth & Design,* vol. 11, pp. 875-1416, 2011.

[13] A. Lewis, M. Seckler, H. Kramer and G. van Rosmalen, Industrial Crystallization: Fundamentals And Applications, Cambridge University Press, 2015.

[14] J. D. Seader, E. J. Henley and D. K. Roper, Separation Process Principles: Chemical And Biochemical Operations, 3rd ed., John Wiley & Sons, Inc., 2011.

[15] N. S. Tavare, Industrial Crystallization: Process Simulation, Analysis And Design, New York: Plenum Publishing Corporation, 1995.

[16] P. Atkins and J. De Paula, Physical Chemistry, 8th ed., vol. 1, Oxford: Oxford University Press, 2006.

[17] M. Sultana, "Microfluidic systems for continuous crystallization of small organic molecules", Massachusetts, 2010.

[18] J. Leng and J.-B. Salmon, "Microfluidic crystallization", *Lab on a Chip,* vol. 9, pp. 24-34, 2009.

[19] C. Rougeot and J. E. Hein, "Application of continuous preferential crystallization to efficiently access enantiopure chemicals", *Organic Process Research & Development,* vol. 19, pp. 1809-1819, 2015.

[20] J. Puigmartí-Luis, "Microfluidic platforms: a mainstream technology", *Chemical Society Reviews,* vol. 43, pp. 2253-2271, 2014.

[21] A. T. Florence and D. Attwood, Physicochemical Principles Of Pharmacy: In Manufacture, Formulation And Clinical Use, Pharmaceutical Press, pp. 8-42, 2015.

[22] M. R. A. Bakar, Z. K. Nagy, A. N. Saleemi and C. D. Rielly, "The impact of direct nucleation control on crystal size distribution in pharmaceutical crystallization processes", *Crystal Growth & Design,* vol. 9, pp. 1378-1384, 2009.

[23] "Mettler Toledo", [Online]. Available: http://www.mt.com/de/en/home/applications/L1_AutoChem_Applications/L2_Crystallization/Supersaturation_Application.html. [Accessed Novembro 2016].

[24] G. S. Bumbrah and R. M. Sharma, "Raman spectroscopy – basic principle, instrumentation and selected applications for the characterization of drugs of abuse", *Egyptian Journal of Forensic Sciences,* vol. 6, pp. 209-215, 2016.

[25] J. C. Edwards, "Process NMR Associates," [Online]. Available: http://www.process-nmr.com/reviewsanddocumentation.html. [Accessed Novembro 2016].

[26] "NIST Livro de Química na Web", [Online]. Available: http://webbook.nist.gov/chemistry/. [Accessed Outubro 2016].

[27] Z. Sun, N. Ya, R. C. Adams and F. S. Fang, "Particle size specifications for solid oral dosage forms: a regulatory perspective", *American Pharmaceutical Review,* vol. 13, pp. 68-73, 2010.

[28] H. Zhang, J. Quon, A. J. Alvarez, J. Evans and A. S. Myerson, "Development of continuous anti-solvent/cooling crystallization process using cascaded mixed suspension, mixed product removal crystallizers", *Organic Process Research & Development,* vol. 16, pp. 915−924, 2012.

[29] J.-R. Wang, B. Zhu, Q. Yu and X. Mei, "Selective crystallization of vitamin D3 for the preparation of novel conformational polymorphs with distinctive chemical stability", *CrystEngComm,* vol. 18, pp. 1101-1104, 2016.

[30] P. Neugebauer and J. G. Khinast, "Continuous Crystallization of Proteins in a Tubular Plug-Flow", *Crystal Growth & Design,* vol. 15, pp. 1089-1095, 2015.

[31] M. Jiang, C. D. Papageorgiou, J. Waetzig, A. Hardy and M. Langston, "Indirect Ultrasonication in Continuous Slug-Flow Crystallization", *Crystal Growth & Design,* vol. 15, pp. 2486-2492, 2015.

[32] M. Jiang, Z. Zhu, E. Jimenez, C. D. Papageorgiou, J. Waetzig, A. Hardy, M. Langston and R. D. Braatz, "Continuous-Flow Tubular Crystallization in Slugs Spontaneously Induced by Hydrodynamics", *Crystal Growth & Design,* vol. 14, pp. 851–860, 2014.

[33] M. Jiang, Z. Zhu, E. Jimenez, C. D. Papageorgiou, J. Waetzig, A. Hardy, M. Langston and R. D. Braatz, "Continuous-flow tubular crystallization in slugs spontaneously induced by hydrodynamics", *Crystal Growth & Design,* vol. 14, p. 851–860, 2014.

[34] M. Jiang, C. D. Papageorgiou, J. Waetzig, A. Hardy and M. Langston, "Indirect ultrasonication in continuous slug-flow crystallization", *Crystal Growth & Design,* vol. 15, pp. 2486-2492, 2015.

[35] P. Neugebauer and J. G. Khinast, "Continuous crystallization of proteins in a tubular plug-flow", *Crystal Growth & Design,* vol. 15, pp. 1089-1095, 2015.

Appendix A Operational temperature of second crystallization stage

The second crystallizer is the second step of the designed unit, which is based on the principle of cooling crystallization (see Section 3.1). The most suitable temperature of this second step should be determined before the optimization of the process (see Section 3.5). Therefore, the continuous crystallization of vitamin D_3 was performed for the following set of temperatures: 10, 7, 5 and 0 ºC, whose results are listed in Table A.1.

Table A.1 Results obtained for the two-stage continuous crystallization performed under the following conditions: temperature of the first crystallizer, 40 ºC; mean residence time in the second crystallizer, 59 s; volumetric flow rate,15 mL h^{-1}; mesh of the filter, 10 μm; configuration of the process, Configuration 1.

		Results*	
Temperature of the 2nd crystallizer (ºC)	**Volume Ratio** (Anti-solvent/Solvent)	**Clogging**	**Crystals present in the Filter**
10	1.5	YES	NO
10	3	YES	NO
0	3	YES	NO
5	3	YES	**YES**
7	3	**NO**	**YES**
7	3	**NO**	NO
7	2	**NO**	**YES**
7	1.5	YES	**YES**

*Red color represents an undesired result and green color represents a desired result.

Appendix B Configuration 1 – Single cycle experiments

Vitamin D_3 can appear in the permeate stream of the filtration dissolved in solution or as small crystals that were not retained in the filter. The mass of the vitamin dissolved in the permeate stream can be determined by its solubility at 7 ºC. The later can be calculated by applying the equation of the solubility curve shown in Figure 3.2:

$$y = 0.0016x^2 + 0.4911x + 15.266 \quad \text{(B.1)}$$

where y corresponds to the vitamin D3 concentration, in mmol L^{-1}, and x corresponds to the temperature, in ºC.

At 7 ºC the concentration obtained is equal to 18.782 mmol L^{-1}. When converting for the unit mg mL^{-1}, the solubility of the vitamin D3 at 7ºC is 7.2 mg mL^{-1}.

If the mass of dissolved vitamin D_3 in the permeate stream is deducted from the feed, it can be observed a substantial increase of the absolute yield of the process (see Table B.1).

Table B.1 Absolute yield of crystallization calculated by excluding the amount of vitamin D_3 dissolved in the permeate stream (i.e., acetonitrile solution).

Volumes ratio (Anti-solvent/Solvent)	**Anti-solvent volume** (mL)	**Feed of vitamin D_3** (mg)	**Mass of vitamin D_3 dissolved in the anti-solvent** (mg)	**Maximum mass of Vitamin D_3 that can crystallize** (mg)	**Absolute yield** (%)	**"Corrected" Absolute yield** (%)
1.5	0.355	25	2.6	22.4	25	28
2	0.473	20	3.4	16.6	31	37
3	0.709	20	5.1	14.9	52	70
4	0.945	20	6.8	13.2	24	36

The "corrected" absolute yield can be determined by the following equations.

$$m_{max} = m_{feed} - V_{AS} \times S_{D_3} \quad \text{(B.2)}$$

$$\eta_{D_3,corrected}(\%) = \frac{\left(m_{feed} \times \eta_{D_3}(\%)\right)}{m_{max}} \quad \text{(B.3)}$$

where m_{max} is the maximum mass of vitamin D_3 that can crystallize, m_{feed} is the vitamin mass that the system is fed up with, V_{AS} is the anti-solvent volume, S_{D_3} is the solubility of vitamin D_3 in acetonitrile, and $\eta_{D_3,corrected}$ is the corrected yield.

Appendix C Configuration 1 – Recycle experiments

C.1. Preparation of feed mixtures

Like the methodology described for the Single cycle experiments (see Section 3.5.1), the Recycle experiments started with the preparation of mixtures composed by vitamin D_3, solvent and anti-solvent. However, these mixtures were only prepared for a volumes ratio of 3 (see Table C.1). For theses mixtures, instead of 20 mg of vitamin, 75 mg were used to obtain a high amount of vitamin D_3 crystals that could be later used for analysis. A filter with a higher surface area was used to avoid an increase in back pressure.

Table C.1 Quantity of each compound for different mixtures with different anti-solvent/solvent volumes ratios.

Anti-solvent/Solvent volumes ratio	**Vitamin D_3 Concentration (mol L^{-1})**	**Vitamin D_3 Mass (mg)**	**Solvent Volume (mL)**	**Anti-solvent Volume (mL)**
3	0.22	75	0.886	2.659

At the end of Cycle 1, as mentioned in Section 3.5.2, the volume of the permeate stream was measured and then the stream was used for the preparation of the feed mixtures of Cycle 2. Considering the volume of the permeate stream, assumed to be the volume of acetonitrile, and the ratio under consideration, it was determined the solvent volume. After, the mass of vitamin D_3 needed for the mixtures was calculated by applying equation 3.2 (see Section 3.5.1). The results for the feed mixtures of Cycle 2 of the two essays performed are presented in Table C.2.

Table C.2 Quantity of each compound for different mixtures with different anti-solvent/solvent volumes ratios.

Anti-solvent/Solvent volumes ratio	**Assay**	**Permeate stream Volume (mL)**	**Solvent Volume (mL)**	**Vitamin D_3 Mass (mg)**	**Vitamin D_3 Concentration (mol L^{-1})**
3	Recycle experiment 1	1.4	0.467	39.49	0.22
	Recycle experiment 2	1.6	0.533	45.13	

C.2. Vitamin D_3 results: mass quantity

The mass of vitamin D_3 obtained in different locations of the system for each cycle of the two essays performed is presented in Table C.3. The mass of vitamin obtained in the permeate stream that is recycled is determined by a mass balance of vitamin D_3 in Cycle 1, and the mass of the feed mixture of Cycle 2 includes the vitamin D_3 of the recycled stream and the one added to prepare the mixture (see Table C.2).

Table C.3 Vitamin D3 mass obtained for the two-stage continuous crystallization performed under the following conditions: temperature of the first crystallizer, 40 ºC; mean residence time in the second crystallizer, 59 s; volumetric flow rate,15 mL h-1; mesh of the filter, 2 μm; configuration of the process, Configuration 1.

			Mass of Vitamin D_3 (mg)					
Anti-solvent/ /Solvent Ratio	**Essay**		**Set-Point**	**Mixture**	**Pumped**	**2nd Crystallizer Precipitate**	**Filter**	**Permeate**
3	Recycle experiment 1	Cycle 1	75.00	74.03	69.71	54.51	8.80	6.40
		Cycle 2	39.49	93.44	89.74	41.10	5.70	25.20
	Recycle experiment 2	Cycle 1	75.00	74.34	72.94	43.04	19.50	10.40
		Cycle 2	45.13	88.15	83.15	46.70	12.70	19.80

According to the methodology presented in Section 3.5.2, the mass percentage of the vitamin in different locations of the system is calculated, which results are presented in Table 4.2 and the results concerning the absolute yield and filter efficiency are presented in Tables 4.3 and 4.4 (see Section 4.1.2).